



## OPEN ACCESS

## EDITED BY

Sjoerd Kluiving,  
VU Amsterdam, Netherlands

## REVIEWED BY

David Kaniewski,  
Université Toulouse III - Paul Sabatier, France  
Harald Stollhofen,  
Friedrich-Alexander-Universität  
Erlangen-Nürnberg, Germany

## \*CORRESPONDENCE

David K. Wright  
✉ david.wright@iakh.uio.no  
Jessica C. Thompson  
✉ jessica.thompson@yale.edu

RECEIVED 30 June 2023

ACCEPTED 05 December 2023

PUBLISHED 05 January 2024

## CITATION

Wright DK, Ivory SJ, Birk JJ, Choi J-H, Davies B, Fiedler S, Davis J, Kaliba P and Thompson JC (2024) Palaeoenvironmental data indicate late quaternary anthropogenic impacts on vegetation and landscapes in Mzimba, northern Malawi. *Front. Environ. Archaeol.* 2:1250871. doi: 10.3389/fearc.2023.1250871

## COPYRIGHT

© 2024 Wright, Ivory, Birk, Choi, Davies, Fiedler, Davis, Kaliba and Thompson. This is an open-access article distributed under the terms of the [Creative Commons Attribution License \(CC BY\)](https://creativecommons.org/licenses/by/4.0/). The use, distribution or reproduction in other forums is permitted, provided the original author(s) and the copyright owner(s) are credited and that the original publication in this journal is cited, in accordance with accepted academic practice. No use, distribution or reproduction is permitted which does not comply with these terms.

# Palaeoenvironmental data indicate late quaternary anthropogenic impacts on vegetation and landscapes in Mzimba, northern Malawi

David K. Wright <sup>1\*</sup>, Sarah J. Ivory <sup>2</sup>, Jago J. Birk <sup>3,4</sup>, Jeong-Heon Choi <sup>5</sup>, Benjamin Davies <sup>6</sup>, Sabine Fiedler <sup>3</sup>, Jacob Davis<sup>7</sup>, Potiphar Kaliba <sup>8</sup> and Jessica C. Thompson <sup>9,10,11\*</sup>

<sup>1</sup>Department of Archaeology, Conservation, and History, University of Oslo, Oslo, Norway, <sup>2</sup>Department of Geosciences, Earth and Environmental Systems Institute (EESI), Penn State University, University Park, PA, United States, <sup>3</sup>Institute of Geography, Johannes Gutenberg-University, Mainz, Germany, <sup>4</sup>Institute of Geography, Georg-August-Universität Göttingen, Göttingen, Germany, <sup>5</sup>Research Center for Geochronology and Isotope Analysis, Korea Basic Science Institute, Ochang, Chungbuk, Republic of Korea, <sup>6</sup>Environmental Studies Program, Tufts University, Medford, MA, United States, <sup>7</sup>Yale University, New Haven, CT, United States, <sup>8</sup>Malawi Department of Museums and Monuments, Lilongwe, Malawi, <sup>9</sup>Department of Anthropology, Yale University, New Haven, CT, United States, <sup>10</sup>Yale Peabody Museum, Yale University, New Haven, CT, United States, <sup>11</sup>Institute of Human Origins, School of Human Evolution and Social Change, Arizona State University, Tempe, AZ, United States

Landscapes are formed by long-term interactions between the underlying geology and climatic, edaphic and biotic factors, including human activity. The Kasitu Valley in the Mzimba District of northern Malawi includes the Kasitu River and its adjacent floodplains and uplands, and it has been a location of sustained human occupation since at least 16 thousand years ago (ka) based on archaeological excavations from rockshelters. We trace the changing ecology and geomorphology of the region through soil stable isotopes ( $\delta^{13}\text{C}$ ,  $\delta^{15}\text{N}$ ), microcharcoal and fossil pollen analysed from alluvial terraces dated by Optically Stimulated Luminescence, and wetland auger cores and archaeological sites dated by radiocarbon. Our results suggest that the region was primarily covered in mosaic forest at ca. 22.5 ka. Middle and Late Holocene samples (6.0–0.5 ka) show an increasingly open, herbaceous landscape over time with an inflection toward more abundant C4 vegetation after 2 ka. Significant upland erosion and terrace formation is also evidenced since 2 ka alongside high concentrations of microcharcoal, suggesting more intensive use of fire. Faecal biomarkers simultaneously indicate higher numbers of humans living adjacent to the archaeological site of Hora 1, which may be indicative of an overall population increase associated with the arrival of Iron Age agropastoralists. More recently, the introduction of exogenous commercial taxa such as *Pinus* sp. are correlated with regional afforestation in our proxy record. These results show increasing stepwise human impacts on the local environment, with deforestation and maintenance of open landscapes correlated with the regional introduction and intensification of agriculture during the Late Holocene.

## KEYWORDS

African Iron Age, erosion, stable isotopes of carbon and nitrogen, organic biomarkers, pollen analysis, archaeoecology, Optically Stimulated Luminescence, human landscape interactions

## 1 Introduction

There is no question that humans have radically changed the complexion of all spheres of Earth's environment. Many scientists have proposed that the significant, irreversible effects of anthropogenesis (human-induced landscape formation) began with the introduction and adoption of formal agricultural techniques in the Holocene (Ellis, 2011; Ruddiman, 2013; Ruddiman et al., 2015). However, there is growing awareness that hunter-gatherers exert significant impacts on ecological systems, and therefore anthropogenesis may extend deeper into the Pleistocene (Boivin, 2016; Roberts et al., 2017; Boivin and Crowther, 2021; Snitker, 2022). In particular, the use of fire (Bird, 2008; Pinter et al., 2011) and extirpation of megafauna (Braje and Erlandson, 2013; van Der Kaars et al., 2017) altered the natural environment in favor of one that was produced by and for human subsistence pursuits. Land use in northern Malawi, as in other rural landscapes in Africa, is predominately agricultural and the ecology of the region has been adapted for that purpose. However, there are many intermediary steps between an ecological system fully adapted to hunting and gathering to one that is fully adapted to farming. Here, we adopt a landscape archaeological approach to study the ecological impacts of climate and human activity on vegetation structure and geomorphology from the Late Pleistocene to Late Holocene of a perennial river valley system in northern Malawi, southern-central Africa. We examine the evolving relationships between human land use and climatic conditions at different points in time and evidence for ecological impacts such as erosion and vegetation change.

The East African Rift System (EARS) and adjacent areas have long been known to be "hotspots" of human occupation because of the topographic variability resulting in precipitation and temperature gradients that are ideal for species adapted for environmental variability such as our own (Potts, 1998). After the emergence of *Homo sapiens*, genetic and linguistic evidence show that as the continent with the longest record of human occupation, it is also the most genetically and linguistically diverse (Beltrame et al., 2016; Vicente and Schlebusch, 2020; Fan, 2023). These long legacies of human innovation, migration, and information sharing have resulted in a variety of landscape management systems that can be examined in a range of environmental settings. Today, this is evidenced by the myriad subsistence practices that are documented across the continent (Garrity et al., 2012), but the roots of these systems extend deep into prehistory and have significantly impacted the formation of present-day ecological systems (Stephens, 2019; Ellis, 2021; Wright, 2022).

Significant questions remain about when and at what scale anthropogenic effects manifested as permanent components of ecosystem functionality in many parts of the world. In northern Malawi, archaeological, geomorphic, and lake core data show that within the last ~85 ka, vegetation changes that followed climate-driven variation were modified by the effects of anthropogenic burning (Thompson et al., 2021). By the terminal Pleistocene, human-influenced landscapes and environments were therefore already well-established through the behaviour of hunter-gatherers, who were then displaced by food producers that migrated into the region by at least 1.7 ka (Juwayeyi, 2011). Along with agriculture and pastoralism, extractive technologies such as pottery production

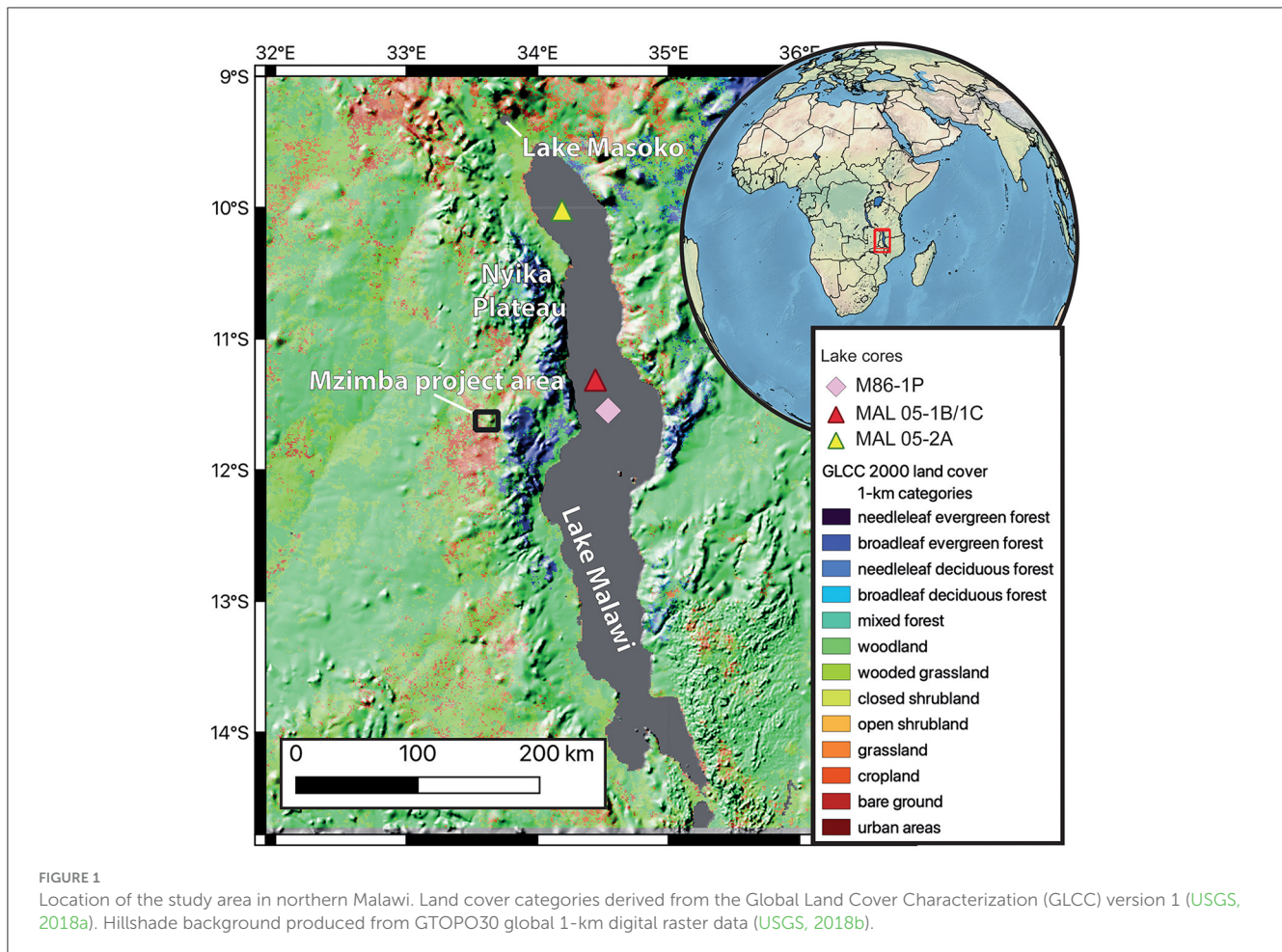
and ironworking would have represented very different modes of land use, and potentially different scales and forms of impacts on environments. Additional migrations into Malawi, documented through archaeology, oral history, and written history, continued throughout the last ca. 0.5 thousand years (kyr) and resulted in new patterns of land use and ecological succession (Thompson, 1981; Juwayeyi, 2020). Increasingly from the mid-1700s, the influence of external economic interests affected patterns of human movement, trade, and resource extraction, particularly ivory and enslaved people (Morris, 2006; Dussubieux et al., 2023). Today, the country is one of the most populous in Africa, and ~56% of the total land is used for agriculture (Li et al., 2017). However, there is little information about the point at which farming technologies transformed the environment through erosion, ecological turnover, and/or establishment of burning ecologies.

Here, we present the results of a combined archaeological-palaeoecological research program from north-central Malawi in which there are human burials dating to at least 16 thousand years ago (ka) (Lipson et al., 2022), although direct evidence for human habitation outside the rockshelters is nearly absent. We seek to identify evidence for ecological "tipping points" (Lenton, 2013; Tylianakis and Coux, 2014; Brovkin et al., 2021) in the past through the study of micro-scale palaeoecological indicators from the landscapes surrounding these archaeological sites. The application of palaeoecological techniques from upland swamps (called *dambos* locally) has opened new possibilities to understand landscape formation processes dating to the same periods of human occupation. By coring, recovering, dating and analysing faecal biomarkers, pollen and light stable isotopes from soil, and studying geomorphic processes on the riverbanks from locations surrounding the rockshelters, we provide insights about the degree of anthropic influence on the formation of the landscape over time.

## 2 Background to the research area

The study region (Figure 1) is located in the humid subtropical climate (Cwa) of south-central Africa (Kottek et al., 2006). The Mzimba District lies on the southern end of the Intertropical Convergence Zone, a pressure meridian extending across the tropics that migrates on an annual basis following the zone of maximum insolation. This creates a strongly bimodal precipitation gradient in this region with high precipitation during the austral summer (December–March) and almost no precipitation during the austral winter (June–September). The annual average precipitation from 1961 to 1990 was 903 mm/yr with an austral winter precipitation averaging <1 mm/month and an austral summer precipitation ranging between 164 and 230 mm/month (NOAA, 2022).

The Lake Malawi region has been subject to climate fluctuations in concert with orbital changes throughout the Quaternary, however, as most of the palaeoenvironmental information comes from drill cores in Lake Malawi, the catchment scale landscape response is not well known. Precipitation reconstructions are regional and suggest climate patterns were driven by a combination of Northern Hemisphere high latitude forcing and local insolation forcing from the late Pleistocene to Holocene (Konecky et al., 2011; Chevalier and Chase, 2015). Landscape formation was, however,



patchy in nature across southern-central Africa. For example, an  $\epsilon_{Nd}$  study of clays from the Zambezi River, which lies over 500 km south of the Mzimba region, shows relatively high discharge during MIS2 relative to MIS3; however, the lowest discharge in the record occurs between 15 and 7 ka (van der Lubbe et al., 2016). On the other hand, studies of lignin phenols, *n*-alkanes, and pollen from a lake core in the northern Lake Malawi basin indicate tree cover from 17 to 13.6 ka and 7.7 to 2 ka, suggesting overall wetter conditions than in the intervening time periods (Castañeda et al., 2009; Ivory et al., 2012). These data correspond to stable isotope values analysed from herbivores from the archaeological site of Makwe, eastern Zambia, which show C3 (woodland) conditions throughout the Holocene followed by C4 (grassy) conditions after 2 ka (Robinson and Rowan, 2017). Similarly,  $\delta D$  *n*-C<sub>31</sub> alkanes from the Zambezi catchment (Schefuß et al., 2011) indicate a regional climatic condition of drier, more open landscapes in the Late Holocene compared to the Middle Holocene. Overall, growing impacts of deforestation and increased warming are reflected in the organic geochemistry of Lake Malawi over the last 700 years (Castañeda et al., 2011), which accords with regional studies such as in the Zambezi catchment, demonstrating the persistence of more open grassland settings, likely as a result of human land use and fire patterns (Burrough and Willis, 2015). Overall, the patterns observed in the proxy record are spatially heterogeneous but show

increasing influences of humans over time that overprint orbitally driven climate cycles.

The research area is situated in the Irumide terrane to the west of the EARS in uplands comprised of Precambrian to Palaeozoic biotite and hornblende rich schists and gneisses to the east, grading to unconsolidated Tertiary and younger sediments to the west and into Zambia (Hopkins, 1973). Residual alluvial and colluvial deposits are found at distal margins of talus slopes that form in response to normal faulting and uplift in the valleys or inselberg outcrops. Sand-rich fluvial terraces draining uplands primarily to the east are found along the margins of the Kasitu River and subordinate drainages and incise older, residual landforms.

Soils in the study area are primarily geogenic and are classified in the Food and Agriculture Organization's World Reference Base for Soil Resources as Rhodic Lixisols and Lixic Ferralsols with the river valley alluvial classified as Ferralic Endogleyic Cambisols (IUSS Working Group WRB, 2015). Lixisols [sometimes called "latosols" and equivalent to Ustalfs in the United States Department of Agriculture (USDA) soil taxonomy; Soil Survey Staff, 1999] generally formed under wetter conditions than present and have been subject to clay eluviation via translocation of fine mineral fraction from the upper to lower aspect of the solum (Ebelhar et al., 2008). Ferralsols (sometimes called "laterites" or "latosols" and equivalent to Oxisols in the USDA soil taxonomy) have high

amounts of kaolinite and iron, aluminum and titanium oxides (Paz et al., 2008). Cambisols (Inceptisols in the USDA soil taxonomy) are poorly developed soils, which, in this setting, have indistinct reddish subsoils forming in alluvium (Chesworth et al., 2008). Overall, the project area is located in a region with patchy suitability for agricultural production, with river valleys hosting the units of land requiring the least intensive dry season efforts at maintaining crops (Li et al., 2017).

The vegetation of the study area is marked by woodlands, grasslands and seasonally flooded grassland swales called *dambos* characteristic of the Sudano-Zambezi region (Werger and Coetzee, 1978). *Dambos* are typically vegetated with *Loudetia simplex*, which flourishes on the clayey soils that build up with annual inundation (Kindt et al., 2014). Surrounding *dambos*, the natural vegetation of the Mzimba District is comprised of *Brachystegia* and *Julbernardia* miombo woodland with grassier occurrences on the Mbelwa Plains to the west (Jackson, 1968). Miombo woodlands are distributed extensively across southern Africa where long dry seasons predominate and include mixed closed and open canopy settings with shallow soils (Frost, 1996). Pollen traps set in the early 1980s on the Nyika Plateau, located ~100 km north of the study region, collected high abundances of herbaceous pollen taxa including Poaceae, Cyperaceae and Apiaceae along with arboreal pollen taxa such as *Olea*, *Juniperus*, and *Podocarpus*, indicating the modern configuration of high-elevation grasslands above ~2000 m above mean sea level (AMSL) with pockets of forest retained between hillslopes (Meadows, 1984b). Pollen from peat cores in *dambos* in the Nyika at the bases of these slopes show that these characteristics were a feature of the region for at least the last 5 kyr, and potentially throughout the Holocene (Meadows, 1984a).

The study area of the Kasitu Valley and adjacent Vipha Uplands ranges from ~1350 to 1750 m AMSL, and as is characteristic of this physiographic region, there is a strong mix of trees (most of which follow a C3 photosynthetic pathway) and grasses (C4 photosynthetic pathway). The degree of openness is influenced by overall rainfall, its seasonal distribution, soil characteristics, and slope aspect (north-facing slopes in the southern hemisphere receive more sunlight, promoting vegetation that can tolerate warmer and/or more xeric conditions). Once more open woodlands are established, they may be maintained through soil compaction that reduces water infiltration and promotes erosion, creating vegetation-landscape feedback loops (Campbell et al., 1995).

Fire also plays an important role in these landscapes of maintaining open vegetation structure. A local study of *Butyrospermum paradoxum* suggests that the evolutionary pathways to fire-dependent germination in the region extend deep into the past and may indicate a long-term relationship between anthropogenic burning and vegetation patterning (Jackson, 1974). Currently, the oldest evidence for human intervention in vegetation character comes from charcoal and pollen records from two deep cores in Lake Malawi, MAL05-2A (near Karonga) and MAL05-1B/1C (near Nkhata Bay), corresponding to changes observed in adjacent archaeological sites entrained within alluvial fans that formed within the last ~100 kyr (Thompson et al., 2021). By ca. 85 ka, overall wetter conditions in the basin were no longer associated with extensive Afromontane forests, and

fire-tolerant taxa had become more common. However, there is less information about local-scale connections between climate, environment, and human behaviour. The terminal Pleistocene and Holocene are not well-studied in the MAL05-1B/1C core that produced records of pollen and charcoal extending beyond 600 ka (Ivory, 2018), but the M96 core from Lake Masoko in southern Tanzania, ~300 km northwest of our study area (Garcin et al., 2007), and the MAL05-2A core from Lake Malawi, ~150 km to the northeast (Ivory et al., 2012), offer basin-scale information about changes in vegetation in northern Malawi during this time. Both cores show an increased seasonal dry forest in the Holocene, with a transition between ca. 14.5 and 11.8 ka toward higher proportions of grassy ground cover at the expense of Afro-montane tree taxa. This is supported by an increase in herbaceous pollen at a comparable depth in the M86-18P core from near Nkhata Bay, ~70 km east of our study area (DeBusk and George, 1998).

Charcoal records from Lake Malawi are not sampled at a fine enough resolution to examine changes in burning regime within the last ca. 18 kyr, the period covering the transition out of the Last Glacial Maximum (LGM), through the terminal Pleistocene, and across the Holocene. Charcoal from Lake Masoko, in southern Tanzania, shows increases in regional fire emissions starting around ca. 1.8 ka, with more input from local fires by ca. 1.5 ka (Thevenon et al., 2003). Between 1.1 – 0.6 ka, a reduction in evidence for fire activity corresponds to a reduction in available fuel load, resulting in vegetation that has potentially been shaped through a series of interactions between climate and human activity (Vincens et al., 2003).

Here, we provide local-scale datasets derived from the late Quaternary terraces of the Kasitu River and a series of *dambos* that provide environmental context for archaeological sites that span over 16 kyr. In the Kasitu Valley today, vegetation is strongly influenced by economic activities such as agriculture and charcoal production. By providing finely resolved local records of environmental and geomorphic change, we demonstrate the antiquity, scale, and consequences of climate and human impacts across four key transitions: (1) LGM to terminal Pleistocene; (2) terminal Pleistocene to Holocene; (3) foraging to food production and (4) globalisation of commerce with the African interior.

## 3 Project description and data collection

### 3.1 Malawi Ancient Lifeways and Peoples Project

The Malawi Ancient Lifeways and Peoples Project (MALAPP) began in 2016 with survey and new excavations at Hora 1 rockshelter (HOR-1, 1470 m AMSL), where two adult human burials were recovered in 1950 (Clark, 1956), and directly dated to ca. 8–9 ka (Skoglund et al., 2017; Lipson et al., 2022). MALAPP excavations in 2019 recovered two infant burials, dated stratigraphically to ca. 14–16 ka (Lipson et al., 2022). All four individuals produced ancient DNA that contributed to discovery of ancient population structure that emerged at the end of the terminal Pleistocene (Skoglund et al., 2017; Lipson et al., 2022).

The total sample of ancient individuals from northern Malawi ( $n = 8$ ) further show that the spread of farmers with western African ancestry into the region during the Late Holocene resulted in genetic replacement of local hunter-gatherer populations (Lipson et al., 2022). The broad context of human occupation in the terminal Pleistocene and Holocene are primarily found at the sites of HOR-1 (ca. >16–8 ka), and three other sites excavated by MALAPP: Hora 5 (HOR-5, 1503 m AMSL, ca. 5–2.6 ka), Kadawonda 1 (KAD-1, 1709 m AMSL, ca. 3.8–1 ka) and Mazinga 1 (MAZ-1, 1401 m AMSL, ca. >9.5–0 ka) (Figure 2). All sites have a small amount of historical and Iron Age material in the uppermost ~10 cm (e.g., Miller et al., 2021; Dussubieux et al., 2023).

MALAPP has prioritised the recovery of ecological datasets to better connect human-environmental processes, but on-site records represent discontinuous blocks of time. To that end, reconnaissance for more continuous and fine-grained sequences of environmental change has been conducted in parallel to the on-site archaeological work since 2017. This work involved collection of soils and sediments from specific geomorphic contexts for the purpose of recovering and identifying stable isotopes of carbon and nitrogen, coprostanol (an organic molecule associated primarily with human faeces) and fossil pollen. We used two primary methods: (1) scraping, drawing profiles and collecting sediments in 100 mL Whirlpaks from excavated or exposed test units on Kasitu River terraces; and (2) utilising a percussion auger to collect polythene cores in 30-cm increments from floodplain and *dambo* (upland wetland) environments. Following the collection of percussion augers, the cores were opened, documented and sampled at the field laboratory of the M'Mbelwa Farm Institute near Lunjika Mission, Malawi. Sediments were then air dried prior to sealing and exporting to the United States, Norway and Germany for analysis.

Locations for auger testing were selected based on the identification of upland swales that were feasible to test and provided spatial context to understand ecological conditions at different distances to known archaeological rockshelter sites. We documented four sedimentologic profiles (sampling three redundantly in 2017 and 2018) and extracted seven percussion augers. Of the percussion auger samples, four were sampled for environmental proxies (fossil pollen, soil stable isotopes, biomarkers). An eighth percussion auger (AU8) was attempted, but the bucket attachment broke, after which a sediment pit (Pit 8) was excavated to retrieve samples for environmental reconstruction.

Locations of ecological proxy collection points were situated in two primary contexts: (1) the Kasitu River valley from sand-rich alluvial terraces dating from 34.6 to 0.5 ka. (2) Three *dambo* upland swale locations with clay-dominant sediments at different distances to the archaeological site of HOR-1. AU7 is situated on the eastern slope of Mount Hora (700 m from the site under excavation). AU8 (Pit 8) is located 4 km west of Mount Hora in an adjacent drainage catchment to HOR-1. This unit is capped by ~50 cm of coarse sands, under which clay-rich *dambo* sediments predominate with the basal 20 cm comprised of sandy loam alluvium. AU3 is located 11.5 km northwest of Mount Hora in a catchment that is not directly connected or adjacent to HOR-1. The purpose of the latter set of samples will be to evaluate land cover changes associated with different scales of human settlement.

## 3.2 Analytical methods

### 3.2.1 Geomorphology, pedology, and sedimentology

Depositional context was first assessed from satellite images, followed by site visits and documentation of exposed or extracted profiles. In the case of terraces along the Kasitu and tributaries, sediment grain sizes and sedimentary structures were noted to infer past fluvial depositional patterns. Soil formation was documented to infer periods of landform stability and weathering features (e.g., redox processes, laterisation) that reflect ground cover and hydrologic conditions. Complete descriptions of the sediment and soil characteristics of the terrace profiles and auger cores *sensu* Schoeneberger et al. (2012) are found in the [Supplementary material](#).

For auger tests, sediments and soils were documented in the field lab after splitting the 30-cm PVC extraction sleeves lengthwise into two halves, undertaking careful documentation of the sediment grain sizes and soil formation features using a hand lens and dental picks, and removing 50–100 g samples from geologically representative locations within the cores believed to be able to reflect changing environmental conditions over the depositional period. Once the cores were split on the laboratory table, samples for stable isotope and organic biomarker analyses were arbitrarily (but systematically) extracted in 2–3-cm thick units from the left side of the core. Between samples, utensils were scrubbed vigorously with sand after which they were washed with clean water and left to air dry in a closed room to avoid contamination. In Oslo, the samples were homogenised together prior to undertaking their respective analytical protocols in Uppsala, Oslo and Mainz (see below). Samples for pollen extraction were removed from the right side of the core, packed into Whirlpaks, and sent to the Ivory Paleoecology Laboratory at the Pennsylvania State University. Utensils were washed with soap and water and air dried in a closed room after every sample.

### 3.2.2 Dating

Determination of ages of sediments and soils from the study locations was undertaken using both radiocarbon ages of organic material or charcoal from the core samples and Optically Stimulated Luminescence (OSL) dating of quartz grains from the terraces. Samples for accelerator mass spectrometry radiocarbon dating were carefully selected using clean dental picks and wrapped in aluminum foil either in the field lab or at the Archaeochemistry Lab of the University of Oslo. Samples from the augers were submitted to the Radiocarbon Laboratory at Uppsala University and have been corrected for isotopic fractionation using the 2020 Southern Hemisphere calibration curve (Hogg et al., 2020). Age-depth models were developed using the “rbacon” package (Blaauw and Christen, 2011) in the R statistical computing environment (v.4.20, R Core Team, 2023), with maximum modelled depths corresponding to the depth of the lowest sample in each sequence (AU3 = 67 cm; AU7 = 77 cm; AU8 = 146 cm).

We collected OSL samples in light-free, 30-cm carbonized steel tubes from the cleaned sidewalls of terrace exposures. The tubes were wrapped in duct tape and transported to the Luminescence Laboratory of the Korea Basic Science Institute in Ochang,

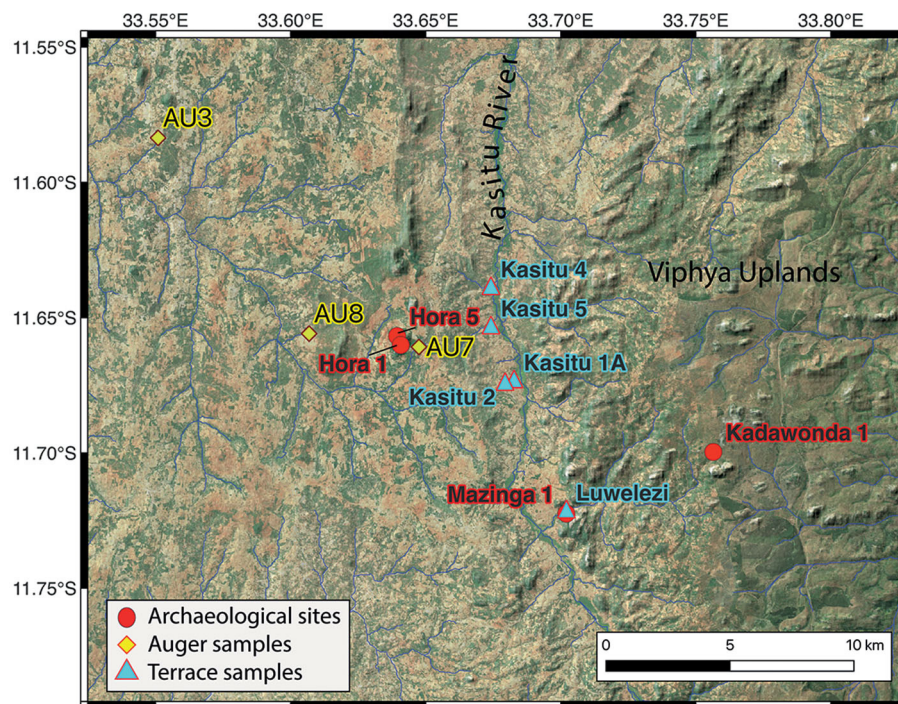


FIGURE 2

The Mzimba project area showing archaeological sites and sampling locations. Image created in QGIS 3.22 with ASTER Global Digital Elevation Model (v3) background downloaded from: <https://earthexplorer.usgs.gov/>. Overlay ESRI panchromatic image obtained from the HCMGIS QGIS plugin.

South Korea, where the sediments were removed and prepared for analysis under low-wavelength light. Grain sizes of 50–180  $\mu\text{m}$  were isolated by density separation, etched with hydrofluoric acid and subjected to Single Aliquot Regeneration of small aliquots (several hundred grains) mounted to 3 mm disks (Bøtter-Jensen et al., 2000; Murray and Wintle, 2003). The calculation of an equivalent dose ( $D_e$ ) involved first measuring discharged radiation (Gy) in a photomultiplier tube after shooting a beam of blue-LED light at irradiated aliquots in a Risø reader (Model TL/OSL-DA-20) fitted with a  $^{90}\text{Sr}/^{90}\text{Y}$  beta radiation source. Samples were then bleached, irradiated, heated and stimulated again with infrared-LED (to remove potential contaminating effects of feldspar inclusions) after which blue-LED stimulation was performed for 40s at 150°C. Dose rates ( $D_r$ ) were determined after calculating secular equilibrium of the sediments using low-level, high-resolution gamma spectroscopy (Liritzis et al., 2013), a cosmic ray dose contribution (Prescott and Hutton, 1994) and the degree of radiation attenuation based on the average water content of the samples over the burial lifetime. For further information, the methods for sample analysis accord with those studied from the nearby Karonga region and published in the Supplementary material of Thompson et al. (2021).

### 3.2.3 Soil stable isotopes

Soil stable isotopes were used to broadly examine the evidence for anthropogenic inputs into sediments ( $\delta^{15}\text{N}$ ) and relative ratios of forest and grass cover ( $\delta^{13}\text{C}$ ) at the sampled locations. Soil nitrogen isotope ratios in non-disturbed ecosystems are generally

inversely correlated with rainfall and temperature, and can thus be used as a general index of aridity (Ambrose, 1991). Plant and soil  $\delta^{15}\text{N}$  values are also consistently higher in anthropogenic sediments (Commisso and Nelson, 2006), particularly during the decomposition of soil organic matter (Natelhoffer and Fry, 1988; Högberg, 1997).

Carbon isotopes in soil are used to identify plant biomass at sampled locations. Carbon isotopes ( $\delta^{13}\text{C}$ ) can be isolated directly from bulk soil matter, reflecting changes in plant spectra based on photosynthetic pathways (C3, C4, CAM) and  $\text{CO}_2$  production (Cerling et al., 1989; Ruiz Pessenda et al., 2009). Such datasets demonstrate relative concentrations of tree (C3) vs. grass (C4) cover (e.g., Srivastava, 2001; West et al., 2006; Ruiz Pessenda et al., 2009) and ability of the soils to store  $\text{CO}_2$  (Bowling et al., 2008; Breecker et al., 2010). In the tropics, C3 plants are generally comprised of trees and leafy dicots and C4 plants tend to be grasses (including sorghum, millets, *Digitaria* sp., African rice and savannah grasses).

Preparation of samples followed protocols outlined in Wright et al. (2019) in which sediments for  $\delta^{13}\text{C}$  analysis were pretreated with 1M HCl for 24h, dried, and then  $25.0 \pm 0.1$  mg were sealed in tin capsules and loaded into a DeltaV Advantage Stable Isotope Mass Spectrometer configured with a Flash Elemental Analyzer (ThermoFisher) for combustion into purified  $\text{CO}_2$  and  $\text{N}_2$  at the CLimate Interpretation of Plant Tissue lab in Department of Biosciences at the University of Oslo. Laboratory precisions were measured between 0.03 and 0.04 per mille (‰) for  $\delta^{13}\text{C}$  using the NBS19 (1.95‰) and LSVEC (−46.6‰) standards as calibrated against a  $\delta^{13}\text{C}_{\text{VPDB}}$  internal standard. Preparation of samples for

$\delta^{15}\text{N}$  followed the same protocols but were not acidified prior to extraction.  $\delta^{15}\text{N}_{\text{AIR}}$  internal references and quality assurance standards were calibrated against USGS40 and USGS41, which have consensus values of  $-4.52$  and  $47.57\%$ , respectively. Precisions were determined to be  $0.1\%$  for the sample runs of  $\delta^{15}\text{N}$ . Statistical treatment of the data include standard ellipses calculated to the  $2\text{-}\sigma$  (95%) level and a loess fit using the “lowess” function and were performed in ggplot2 in RStudio 2022.07.1 (Build 554). All data and code are available at: <https://doi.org/10.6084/m9.figshare.23092127>.

### 3.2.4 Organic biomarkers

Faecal stanols are organic molecules produced in the guts of mammals, most especially humans who produce high amounts of coprostanol; they can be used to detect relative population sizes on a landscape level (Bethell et al., 1994; Bull et al., 2002; Evershed, 2008; Zocatelli et al., 2017). High levels of coprostanol are also found in the faeces of non-human primates and pigs (family Suidae), but most data show that coprostanol does not dominate the biomarker spectrum here as much as in human faeces (Subbiah et al., 1972; Ausman, 1993; Shah, 2007; Sistiaga, 2015; Prost, 2017; Zocatelli et al., 2017). Faeces of herbivores contain less coprostanol than humans but higher amounts of  $5\beta$ -stigmastanol, providing opportunities to reconstruct the demography of both humans and ruminant animal communities (Prost, 2017). Bile acids are an important companion biomarker to stanols because they allow a differentiation between primate faeces, the faeces of pigs and distinct herbivores (Prost, 2017; Zocatelli et al., 2017). *n*-Alkanes are found in the epicuticular layer of leaves and can be used to distinguish litter input from grasses and herbs from broadleaf trees (Eglinton and Hamilton, 1967; Zech et al., 2010; Bush and McInerney, 2013).

Faecal biomarkers and *n*-alkanes were extracted in tandem with stable isotopes following sample homogenisation. Biomarkers were extracted by a total lipid extract in a microwave oven after which the method of Birk (2012) was used for purification and derivatisation with small modifications. The extract was saponified and the biomarkers were recovered from the saponification solution by a sequential lipid-lipid extraction. During this step the bile acids were separated from the other biomarkers. The bile acids were purified by solid phase extraction after methylation. Stanols,  $\Delta^5$ -sterols and *n*-alkanes were separated and purified by a solid phase extraction, which yielded *n*-alkanes and steroids in different fractions.

Steroids were measured by gas chromatography mass spectrometry after silylation (GC/MS; 7000D MS connected to a 7890B GC equipped with a DB-5ms Ultra Inert column, Agilent, Santa Clara, CA, USA) and *n*-alkanes by gas chromatography flame ionization (GC-FID; 7890B GC equipped with a HP5 column, Agilent, Santa Clara, CA, USA). Detailed descriptions of the analytical procedures and data outputs are provided in the [Supplementary material](#).

### 3.2.5 Pollen analysis

Fossil pollen and microscopic charcoal analyses of *dambos* and terraces were conducted to reconstruct vegetation and regional-scale fire in the past. All samples were processed using standard pollen extraction methods, including digestion of silicates by

hydrofluoric acid and removal of organics by acetolysis (Fægri et al., 1989). Following completion of the 2017 field season, terrace samples were sent to LacCore Facility at the University of Minnesota for processing. During the extraction phase, a contaminated batch of microspheres was added to a single batch of samples (8). For these samples, it was not possible to calculate charcoal concentrations, and thus microcharcoal is not presented for these samples only. For the 2019 season, the auger samples were processed at Penn State University. These were sieved at 10 microns to remove clays, and *Lycopodium* spores were added to calculate concentrations of pollen and charcoal.

Where possible, over 300 pollen grains were counted per sample; however, preservation of pollen was particularly poor in samples from AU8 and AU3-3. For these samples, pollen counts were significantly lower, ranging from completely sterile to 57 grains. Samples from these augers are interpreted qualitatively. The record comprised 49 pollen and plant spore taxa and 5 morphotypes of fungal spores (including *Sporormiella*). Atlases of pollen morphology were used for identifications (Maley, 1970; Bonnefille and Rioulet, 1980) as well as the African Pollen Database (<https://africanpollendatabase.ipsl.fr>). For the terrace samples only, bisaccate grains of *Podocarpus* and *Pinus* were not differentiated, thus this group is presented as Pinopsida undifferentiated. This only influences the youngest terrace samples, as *Pinus* was introduced to the region in the twentieth century. Pollen abundances are calculated based on a sum of all pollen and plant spores excluding broken grains and aquatics (Cyperaceae, *Typha*). Pollen diagrams were produced using the “rioja” package (v.1.0–5, Juggins, 2022) in R (v.4.20, R Core Team, 2023). Terrestrial pollen taxa are presented as a percentage of all terrestrial plants; aquatic pollen taxa are presented as percentage of combined terrestrial and aquatic plants. Cases where values are consistently lower than 5% include a  $5\times$  exaggeration (lighter shading).

Microcharcoal was differentiated into two categories based on aspect ratios (length/width). Following methods presented in Miao et al. (2019) and Feakins et al. (2020), particles with higher aspect ratios (length/width > 2.5) have been associated with the burning of grass or sedge, while those with lower aspect ratios are associated with burned woody material. All data and code are available at: <https://doi.org/10.6084/m9.figshare.23092127>.

## 4 Results

### 4.1 Sedimentation

Radiocarbon (Table 1) and OSL (Table 2) ages from the *dambo* and terrace sequences, respectively, situate the environmental and archaeological sequences of the present study to beginning in the Late Pleistocene and continuing through into the late twentieth century CE. Sediment cores extracted from wetland environments and pits excavated into terraces of the Kasitu River exposed in secondary drainageways demonstrate relatively slow sedimentation from the Pleistocene to the Middle Holocene (Figures 3, 4). Three profiles with coverage from this time period with absolute ages show accumulation rates from 19.0 to 8.6 ka (AU8) of 0.07 mm/yr, 0.09 mm/yr (Kasitu 4, 135 cm between 34.6 and 18.8 ka), and 0.25 mm/yr (Kasitu 2, 90 cm between 7.1 and 3.5 ka).

TABLE 1 Radiocarbon ages from environmental sampling of the Mzimba District, Malawi.

Lab #	MALAPP code	Corresponding proxy (Figure 3)	Material	$\delta^{13}\text{C}$	$^{14}\text{C}$ age	2- $\sigma$ cal yr BP
Ua-69522	ISO29	POL31	Fine sandy loam	-16.2	15742 $\pm$ 59	18850-19111
Ua-69523	ISO31	POL33	Clay	None	7759 $\pm$ 124	8223-8984
Ua-69524	ISO33	POL35	Coarse sandy loam	-23.7	1794 $\pm$ 32	766-921
Ua-69525	ISO42	POL36	Clay loam	-16.2	101.8 $\pm$ 0.3*	AD 1958-2000
Ua-69526	ISO45	POL39	Fine sandy clay loam	-16.9	792 $\pm$ 27	657-728
Ua-69527	ISO47	POL41	Silt loam	-17.1	1233 $\pm$ 28	989-1179
Ua-69528	ISO48	POL42	Silt loam	-18.1	927 $\pm$ 28	727-904
Ua-69529	ISO50	POL44	Fine sandy loam	-10.5	2388 $\pm$ 37	2153-2680
Ua-69824	ISO8	POL8	Silt loam	-15.3	964 $\pm$ 29	766-921
Ua-69825	ISO9	POL9	Clay loam	-14.8	267 $\pm$ 29	146-433
Ua-69826	ISO10	POL10	Clay loam	-14.6	49 $\pm$ 29	Suess effect
Ua-69827	ISO11	POL11	Clay loam	-16.8	104.0 $\pm$ 0.4*	AD 1958-1999
Ua-69828	ISO30	POL32	Clay	-16.2	9690 $\pm$ 51	10744-11200
Ua-69829	ISO43	POL37	Clay loam	-15.9	149 $\pm$ 29	Suess effect
* <i>pMC</i>						

Radiocarbon ages calendar corrected for atmospheric production of radiocarbon (Hogg et al., 2020) in OxCal 4.4. Samples Ua-69525 and Ua-69827 were calibrated using the Calib post-bomb correction curve (<http://calib.org/CALIBomb/>) and reported in years AD.

However, accumulation rates for sections with absolute ages after the Middle Holocene are much greater. The Luwezi profile (247 cm of deposition between 1.2 and 0.2 ka = 2.47 mm/yr) has multiple inferred periods of landscape stabilisation based on palaeosol formation, and Kasitu 5 (130 cm of deposition but two indistinguishable ages within the 1- $\sigma$  statistical error of 0.4  $\pm$  0.02 ka, has two inferred periods of landscape stabilisation. Sediment cores with radiocarbon ages (AU3, AU7) also show accumulation rates >1 mm/yr after 1 ka. The historical deposition and erosion rate is also supported through conversations with local farmers and lifelong residents; for example, one informant described a time about ca. 2010-2015 when he could see large cobbles at the base of the Luwezi stream. Today, this tributary to the Kasitu is a flat-bottomed and silty perennial waterway. Examples of recent erosion are clearly observable in road and water cuts, including some with pottery sherds buried under more than 1 m of sediment.

## 4.2 Stable isotopes

Light stable isotopes ( $\delta^{13}\text{C}$ ,  $\delta^{15}\text{N}$ ) extracted from sediments and soils show an inverse correlation between  $^{13}\text{C}$  and  $^{15}\text{N}$  (Supplementary Table 1; Figure 5). Uneven coverage of radiometric ages and variable preservation of nitrogen in the sediments obfuscates time-transgressive correlations of carbon and nitrogen isotopes. However, plotting of  $^{13}\text{C}$  values using stratigraphic inference with ages shows increasingly heavier isotopic composition over time with a relatively unchanging value of  $\sim$ -22‰ spanning from ca. 8-2.5 ka and rapid isotopic enrichment thereafter relative to the preceding ca. 20 kyr (Figure 6).

## 4.3 Biomarkers

AU7 was analysed quantitatively for *n*-alkanes, faecal bile acids and faecal stanols as well as related steroids (Tables 3, 4; Figure 7). Long-chain *n*-alkanes (C26-C33) had concentrations of  $\leq$ 40  $\mu\text{g/g}_{\text{TOC}}$  (Table 3), the faecal 5 $\beta$ -stanols had concentrations  $\leq$ 4  $\mu\text{g/g}_{\text{TOC}}$ , the precursor substances of these biomarkers,  $\Delta^5$ -sterols, had concentrations  $\leq$ 141  $\mu\text{g/g}_{\text{TOC}}$  and 5 $\alpha$ -stanols, the reduction products of  $\Delta^5$ -sterols, which are formed in the environment outside of the gut of mammals, had concentrations  $\leq$ 38  $\mu\text{g/g}_{\text{TOC}}$  (Table 4 and Supplementary Table 4). Bile acids had concentrations  $\leq$ 14  $\mu\text{g/g}_{\text{TOC}}$  (Supplementary Table 5).

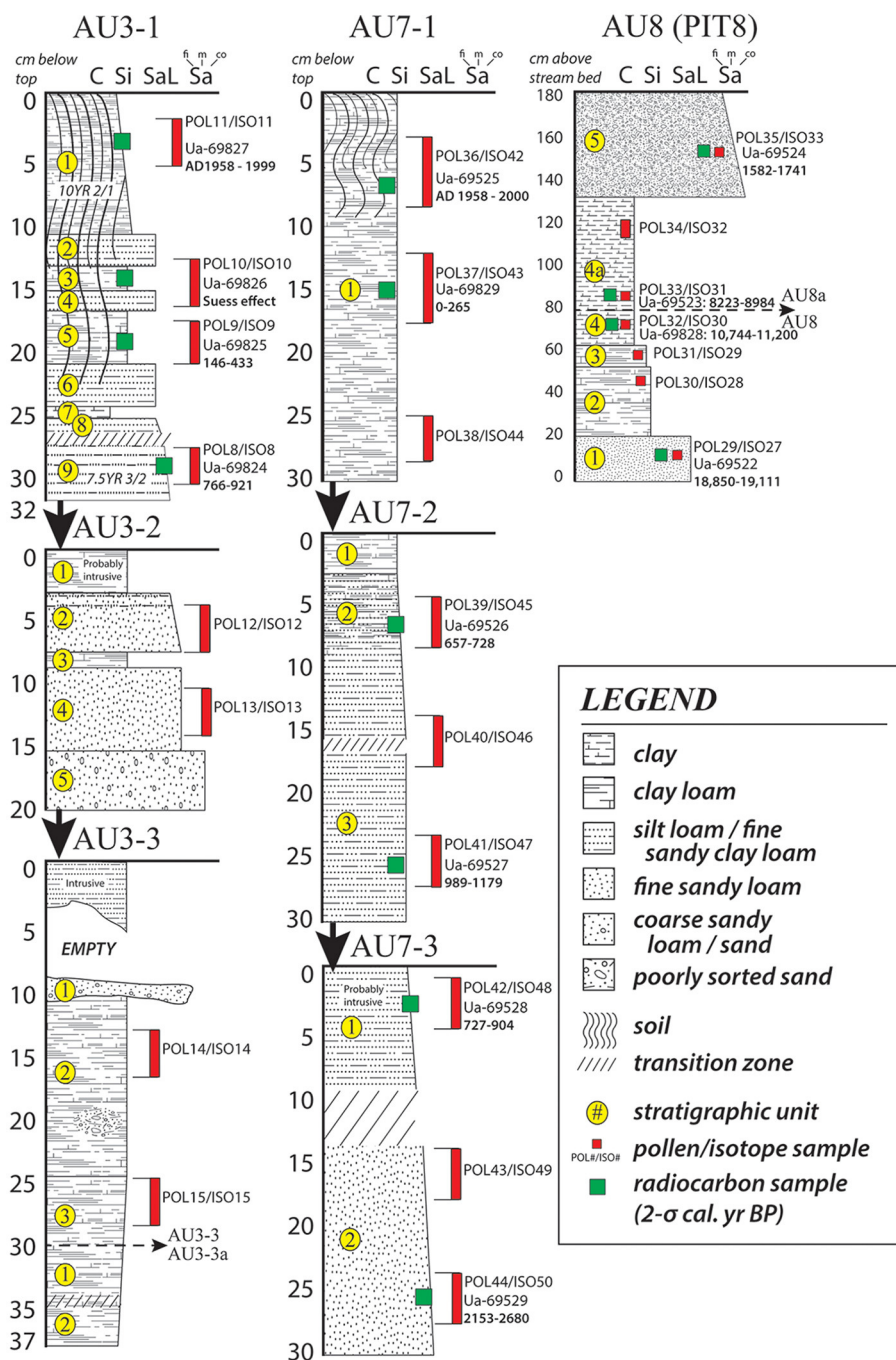
The ratio of the concentrations of long-chain *n*-alkanes with odd numbers of carbon vs. long-chain *n*-alkanes with even numbers of carbon [odd-over-even predominance; OEP; (C27 + C29 + C31 + C33)/(C26 + C28 + C30 + C32)] can be used to identify higher plant biomass inputs into sediments as well as determining the degree of degradation of *n*-alkanes (Eglinton and Hamilton, 1967; Hoefs et al., 2002; Zech and Glaser, 2008; Buggle et al., 2010; Bush and McInerney, 2013). Ratios  $\geq$  4 are characteristic for *n*-alkane inputs from higher biomass plants (Hoefs et al., 2002; Zech and Glaser, 2008). Only the lowermost sample and the uppermost sample from AU7 (ISO50 at -80.5 cm dating to ca. 2.3 ka and ISO42 at -2.5 cm dating to AD1958-2000) had an OEP value <4 (Table 3) indicating dominance of aquatic or degraded *n*-alkanes. These samples were therefore excluded from the following consideration of the terrestrial inputs of plant biomass. All other samples had OEP values  $\geq$ 6 (Table 3). Chain lengths C27 and C29 are the dominant chain lengths in broadleaf trees, and chain lengths C31 and C33 have a high abundance in grasses and other herbaceous plants (Buggle et al., 2010; Zech et al., 2010; Bush



TABLE 2 Optically Stimulated Luminescence ages from environmental context sampling of the Mzimba District, Malawi (Figure 4).

Sample; Sample loc.	Depth (cm) $\bar{x}$	Water content <sup>†*</sup> (wt. %)	<sup>238</sup> U (Bq·kg <sup>-1</sup> )	<sup>226</sup> Ra (Bq·kg <sup>-1</sup> )	<sup>232</sup> Th (Bq·kg <sup>-1</sup> )	<sup>40</sup> K (Bq·kg <sup>-1</sup> )	Dry beta <sup>a</sup> (Gy·ka <sup>-1</sup> )	Dry gamma <sup>a</sup> (Gy·ka <sup>-1</sup> )	Cosmic ray <sup>b</sup> (Gy·ka <sup>-1</sup> )	Total dose rate (Gy·ka <sup>-1</sup> )	D <sub>e</sub> (Gy)	n	Age <sup>c</sup> (ka)
MAL17-1; Kasitu 1A	75	4 ± 1	32.9 ± 8.3	26.3 ± 0.6	91.5 ± 3.1	831 ± 14	2.91 ± 0.11	1.97 ± 0.04	0.22 ± 0.02	4.88 ± 0.12	11.4 ± 0.5	16	2.3 ± 0.1
MAL17-2; Kasitu 1A	25	3 ± 1	15.9 ± 8.2	24.5 ± 0.6	91.9 ± 3.1	962 ± 16	3.17 ± 0.12	2.06 ± 0.04	0.25 ± 0.02	5.30 ± 0.12	7.2 ± 0.4	16	1.4 ± 0.1
MAL17-3; Kasitu 2	155	3 ± 1	26.6 ± 7.2	30.4 ± 0.6	116.9 ± 3.6	1068 ± 16	3.65 ± 0.13	2.50 ± 0.04	0.19 ± 0.02	6.14 ± 0.14	43.5 ± 2.0	16	7.1 ± 0.4
MAL17-4; Kasitu 2	65	3 ± 1	32.0 ± 9.5	32.8 ± 0.7	141.7 ± 4.4	1168 ± 19	4.08 ± 0.15	2.90 ± 0.05	0.23 ± 0.02	6.94 ± 0.16	24.2 ± 1.3	14	3.5 ± 0.2
MAL17-6; Kasitu 4	235	2 ± 1	43.3 ± 7.7	27.9 ± 0.6	77.6 ± 2.7	479 ± 10	2.02 ± 0.08	1.54 ± 0.03	0.17 ± 0.02	3.63 ± 0.09	125.7 ± 5.9	15	34.6 ± 1.8
MAL17-7; Kasitu 4	100	8 ± 2	53.1 ± 6.0	41.7 ± 0.6	114.1 ± 3.5	545 ± 10	2.51 ± 0.09	2.14 ± 0.05	0.21 ± 0.02	4.45 ± 0.11	83.8 ± 2.6	11	18.8 ± 0.8
MAL17-8; Luwelezi	315	14 ± 3	23.5 ± 7.8	11.6 ± 0.6	78.1 ± 2.8	621 ± 12	2.20 ± 0.09	1.54 ± 0.03	0.15 ± 0.01	3.34 ± 0.11	4.0 ± 0.1	15	1.2 ± 0.1
MAL17-9; Luwelezi	130	5 ± 1	5.9 ± 60.6	7.6 ± 0.6	43.6 ± 2.	767 ± 14	2.24 ± 0.09	1.20 ± 0.02	0.20 ± 0.02	3.46 ± 0.09	2.3 ± 0.3	14	0.7 ± 0.1
MAL17-10; Luwelezi	68	3 ± 1	2.4 ± 2.4	4.0 ± 0.5	20.2 ± 1.5	715 ± 16	1.91 ± 0.07	0.84 ± 0.02	0.23 ± 0.02	2.89 ± 0.08	0.6 ± 0.1	12	0.2 ± 0.0(1)
MAL17-11; Kasitu 5	190	4 ± 1	1.4 ± 5.3	14.1 ± 0.6	41.6 ± 2.1	1054 ± 22	2.92 ± 0.11	1.44 ± 0.03	0.18 ± 0.02	4.35 ± 0.12	1.6 ± 0.1	15	0.4 ± 0.0(2)
MAL17-12; Kasitu 5	60	3 ± 1	40.2 ± 6.5	31.9 ± 0.7	122.8 ± 4.6	560 ± 15	2.49 ± 0.10	2.19 ± 0.05	0.23 ± 0.02	4.76 ± 0.11	1.9 ± 0.1	12	0.4 ± 0.0(2)

<sup>‡</sup>Depths of the samples are the vertical distance from the modern ground surface. <sup>\*</sup>Present water contents ( $\pm 20\%$  of uncertainty). <sup>a</sup>Data from high-resolution low level gamma spectrometer were converted to infinite matrix dose rates using conversion factors given in Liritzis et al. (2013). <sup>b</sup>Cosmic ray dose rates were calculated using the equations given by Prescott and Hutton (1994). <sup>c</sup>Central age  $\pm 1\sigma$  standard error. The targeted mineral was quartz with diameters of 90-250  $\mu\text{m}$ . Measurement mode: SAR protocol, preheat at 240 °C (samples KT2992, 2995, 2996, 2997, 2998, 2999) or 260 °C (samples KT2988, 2989, 2990, 2991, 2993, 2994) for 10 s, multiple grain single aliquots (three 8 mm aliquots for each sample).



**FIGURE 3** Schematic profiles of wetland auger tests from the Mzimba region, Malawi showing sedimentation, soil development, and the locations where samples were taken from the cores. AU3 and AU7 were extracted in sequences using a percussion auger to access deeper aspects of the landform until refusal occurred. Sediment and soil classification schemes follow the USDA standards as outlined in Schoeneberger et al. (2012).

and McInerney, 2013). The ratios of the *n*-alkanes C27 and C29 to the *n*-alkane C33 are therefore high with an input of litter originating from deciduous trees and low with an input of biomass originating from grasses. *n*-Alkane ratios (C27/C33 = 0.2 and C29/C33 = 0.9, Figure 6) indicate a strong decrease in forest cover from ISO47 at -53 cm (ca. 1 ka) relative to the underlying (earlier) samples (C27/C33 ≥ 0.3 and C29/C33 ≥ 1.1; Figure 7; Supplementary Table 3).

ISO47 further shows high concentrations of the faecal biomarkers coprostanol (5β-cholestan-3β-ol; 1.4 μg/g<sub>TOC</sub>) and epi-coprostanol (5β-cholestan-3α-ol; 1.3 μg/g<sub>TOC</sub>), indicative of the presence of omnivores such as humans, non-human primates or pigs (Table 4). However, other stanols had also high concentrations at this depth (Table 4) and background values of faecal biomarkers were found in soils and sediments where no enhanced deposition of faeces was assumed (Bethell et al., 1994; Evershed et al., 1997;

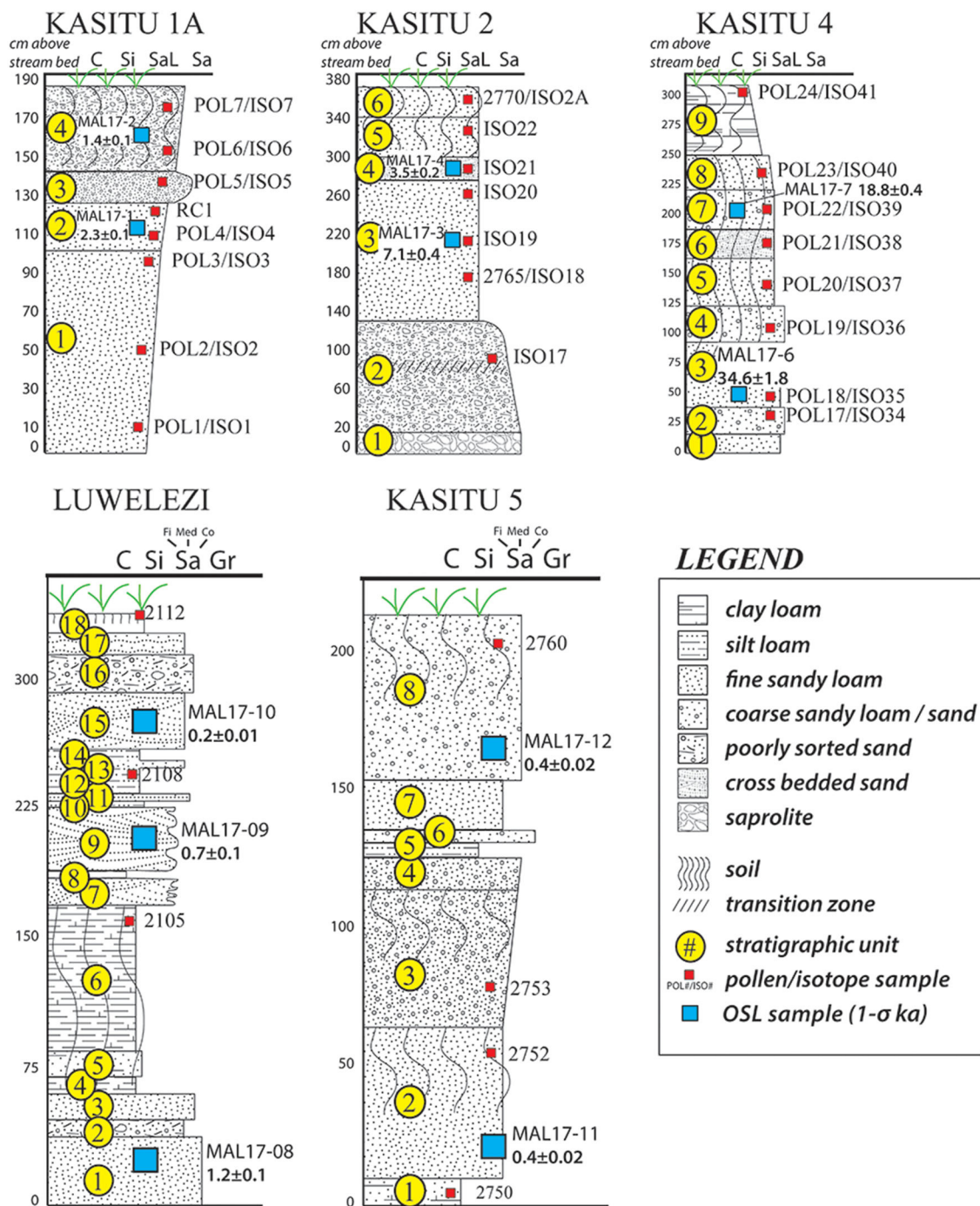
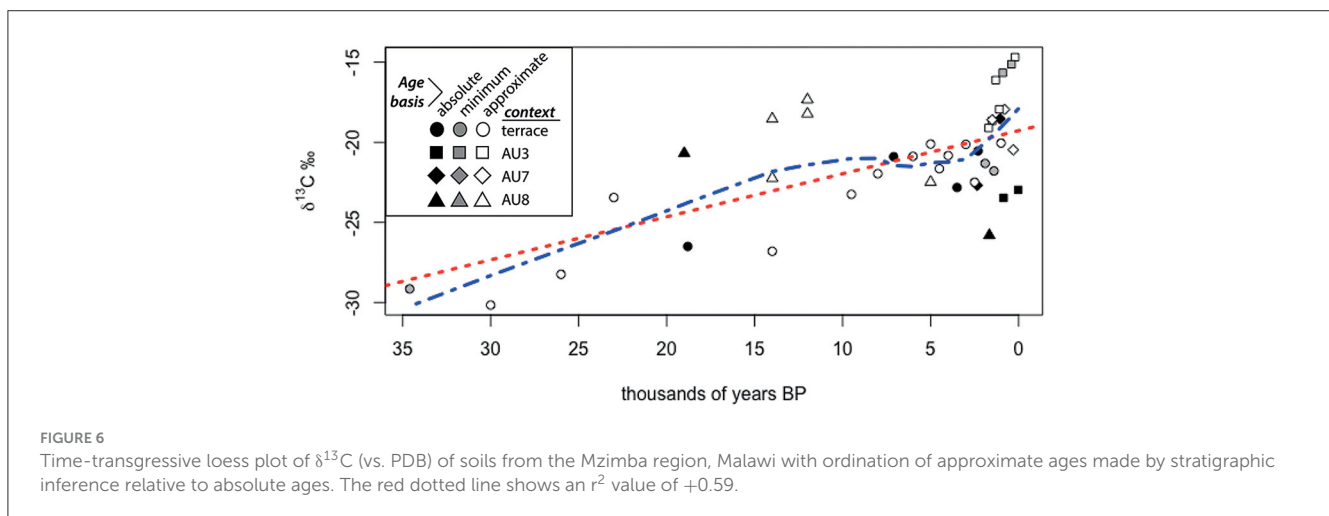
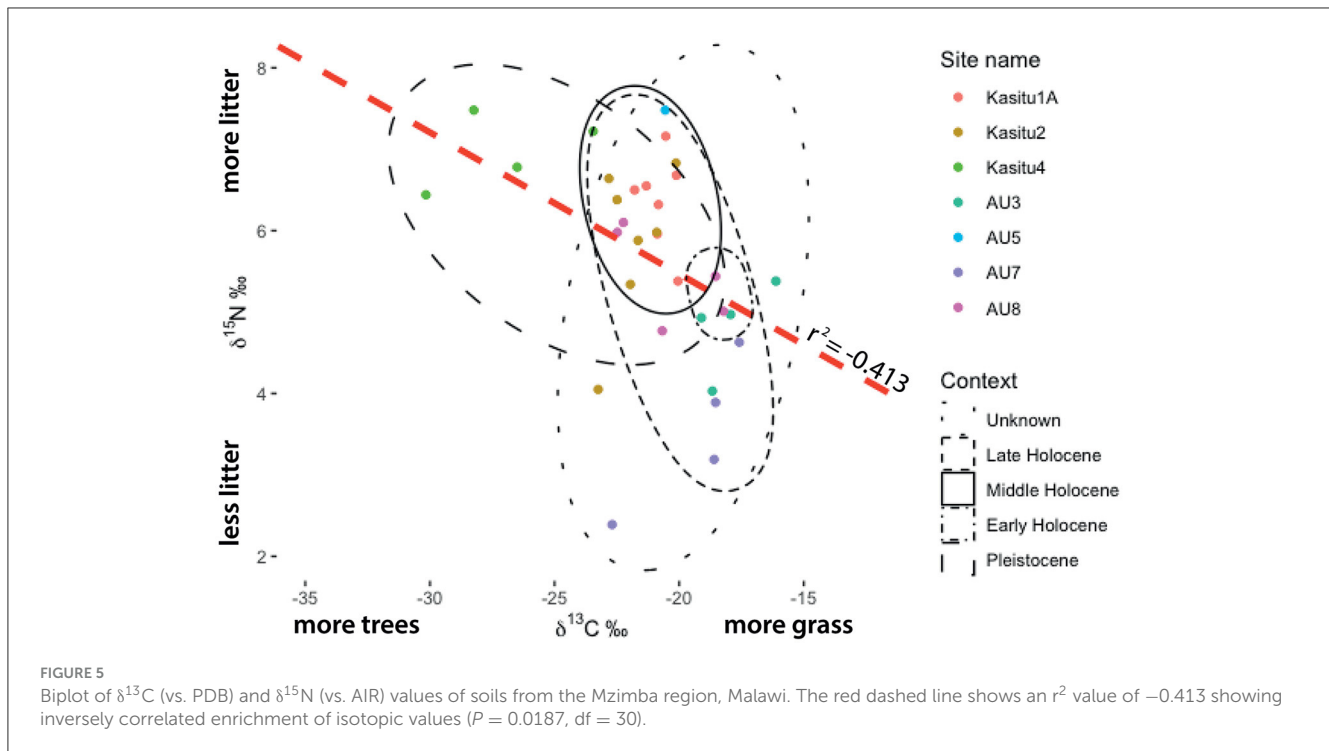


FIGURE 4 Schematic profiles of alluvial terraces from the Mzimba region, Malawi showing sedimentation, soil development and the locations where samples were taken from the profiles. Sediment and soil classification schemes follow the USDA standards as outlined in Schoeneberger et al. (2012).

Bull et al., 2001). To correct for these background values, the amounts of coprostanol and its epimer were related to the amounts of cholestanol ( $5\alpha$ -cholestan- $3\beta$ -ol), which is the reduction product of cholesterol ( $\Delta^5$ -sterol) that is mainly formed outside of the gut of mammals ([coprostanol + epi-coprostanol]/cholestanol, Bull et al., 2002). This ratio showed high values in ISO47 (0.3) in relation to the other samples indicative for faeces inputs

(Figure 7). Although coprostanol and its epimer can also be found in the faeces of herbivores, the more specific biomarkers for faeces of herbivores are  $5\beta$ -stigmastanol ( $5\beta$ -stigmastan- $3\beta$ -ol) and epi- $5\beta$ -stigmastanol ( $5\beta$ -stigmastan- $3\alpha$ -ol), which are the reduction products of phytosterols, due to the high concentrations of the phytosterols in their diet (Leeming et al., 1996; Tyagi et al., 2008; Gill et al., 2010; Prost, 2017). The ratio (coprostanol



+ epi-coprostanol)/(5 $\beta$ -stigmastanol + epi-5 $\beta$ -stigmastanol) was calculated to differentiate between faeces of omnivores and herbivores (high values indicate higher inputs of omnivorous faeces and lower by inputs of herbivorous faeces). This ratio also had a high value in ISO47 (0.5, Table 4). The bile acid patterns of AU7 showed a dominance of deoxycholic acid, the presence of lithocholic acid and the absence of hyodeoxycholic acid (Supplementary Table 5). Therefore, the omnivorous faeces were likely derived from primate sources rather than pigs (Tyagi et al., 2008; Prost, 2017). The more pronounced domination of coprostanol in the biomarker patterns of human faeces in relation to non-human primate faeces (Subbiah et al., 1972; Ausman, 1993; Shah, 2007; Sistiaga, 2015; Prost, 2017; Zocatelli et al., 2017), and the close proximity of the test site to the Hora 1 archaeological site,

which is densely packed with anthropogenic refuse, suggests that the faeces derived from omnivores was most likely from humans.

Between  $-44\text{ cm}$  (ISO46) and  $-34\text{ cm}$  (ISO45 dating to 0.7 ka), there is an increase in forest cover indicated by an increase in C27/C33 ratios to 0.4 and C29/C33 to 1.0 (Figure 7). However, alkane ratios in ISO45 were still lower than in the period before the forest decrease shown in the lower samples (ISO49). This period of afforestation is succeeded by an indication of a decrease in forest cover at  $-26\text{ cm}$  (ISO44) based on C27/C33 ratios of 0.2 and C29/C33 to 0.4, coupled with high values of the ratios that are indicative for omnivorous faeces [(coprostanol + epi-coprostanol)/(5 $\beta$ -stigmastanol + epi-5 $\beta$ -stigmastanol) of 0.3; Figure 7 and Table 4]. The sample above

TABLE 3 Quantities of long chain *n*-alkanes ( $\mu\text{g/g}_{\text{TOC}}$ ) and odd-over-even predominance [OEP (C27 + C29 + C31 + C33)/(C26 + C28 + C30 + C32)] from AU7, Mzimba region, Malawi.

Sample number	Mean depths (cm)	C26	C27	C28	C29	C30	C31	C32	C33	OEP
		( $\mu\text{g/g}_{\text{TOC}}$ )	( $\mu\text{g/g}_{\text{TOC}}$ )	( $\mu\text{g/g}_{\text{TOC}}$ )	( $\mu\text{g/g}_{\text{TOC}}$ )	( $\mu\text{g/g}_{\text{TOC}}$ )	( $\mu\text{g/g}_{\text{TOC}}$ )	( $\mu\text{g/g}_{\text{TOC}}$ )	( $\mu\text{g/g}_{\text{TOC}}$ )	
ISO42	2.5	31	26	25	23	14	30	11	37	1
ISO43	15	2	7	2	16	2	20	2	38	9
ISO44	26.25	4	6	3	14	2	15	2	33	6
ISO45	33.75	3	10	3	23	2	19	3	24	7
ISO46	44	4	8	5	31	4	24	2	36	7
ISO47	53	4	8	4	34	3	22	5	39	7
ISO48	58	2	9	3	36	4	26	3	32	9
ISO48	58	2	9	5	37	2	30	<LOQ	29	11
ISO49	69.75	0	7	4	16	4	16	<LOQ	10	6
ISO50	80.5	6	5	5	14	0	13	<LOQ	<LOQ	3

LOQ, limit of quantification.

(ISO43) dates to within the last 300 years and shows stability in grass vs. trees present on the landscape. The penultimate sample (ISO42) showed high quantities of several steroids but the stanol ratios did not show especially enhanced input of omnivorous faeces [(coprostanol + epi-coprostanol)/cholestanol of 0.1 and (coprostanol + epi-coprostanol)/(5 $\beta$ -stigmastanol + epi-5 $\beta$ -stigmastanol) of 0.2; Figure 7, Table 4, and Supplementary Table 4]. A full data presentation of the results of biomarker analyses are found in the Supplementary material.

#### 4.4 Pollen reconstruction

Fossil pollen concentrations were generally high in the auger samples (6,327 grains/cm<sup>3</sup>), apart from augers AU3-3 and AU8 (average = 447 grains/cm<sup>3</sup>). AU3-3 was sterile except for a few poorly preserved pollen grains and will not be discussed in the results. Within samples where 300 grains counts were achieved, broken, and/or crumbled grains were generally low (<3.5%; Figure 8).

AU8 was a core from ~1360 m AMSL in an open swale surrounded by woodland about 8 km west of the Kasitu River and 3.75 km west of the HOR-1 site. It is not presently under cultivation. The oldest samples in this unit are late Pleistocene (ca. 19 ka) and extend to the late Holocene (1.6 ka). Pollen concentrations were low in these samples (average = 656 grains/cm<sup>3</sup>); however, pollen was observed in all samples and as these include some of the oldest dated samples in our record, we report here the qualitative presence of key pollen taxa. Overall, these samples were dominated by Poaceae pollen, while other herbs like Asteraceae were consistently present. Cyperaceae pollen was generally near the lowest values of all pollen samples in this interval (mean = 22.5%) and tree pollen presence was sporadic.

AU7 was a core from ~1425 m ASML in a sparsely wooded grassy swale about 3.75 km west of the Kasitu River and 0.6 km southeast of the HOR-1 site. This site is not presently under

agriculture. These samples cover ca. 2.6 kyr of the late Holocene and were recovered from a *dambo* wetland that is subject to slow, seasonal sedimentation. These samples were dominated throughout by aquatic pollen taxa such as Cyperaceae (mean = 212% relative to the terrestrial pollen sum), in particular *Ascolepis* (mean = 36%; Cyperaceae family). Of the terrestrial pollen taxa, Poaceae reached maximum values in a sample dated to 0.8 ka, then decreased minimally until present. Tree pollen was present in the pre-modern samples in lower abundances (8%) until an increase in *Podocarpus* and *Pinus* in the most recent two samples (24%, 5%). Microcharcoal increased from the pre-modern (mean = 11,617 particles/cm<sup>3</sup>) to the modern samples (mean = 106,499 particles/cm<sup>3</sup>), with charcoal with high aspect ratios indicating a grassy source dominating.

AU3 was a core from ~1320 m ASML in a seasonally flooded grassland about 12 km west of the Kasitu River and 11.5 km northwest of the HOR-1 site. It is not presently under agriculture and is surrounded by dense woodland. These samples cover ca. 1 kyr of the Late Holocene and were dominated by aquatic pollen taxa like Cyperaceae (mean = 133% relative to the terrestrial pollen sum), especially *Ascolepis* (17%). Of the terrestrial pollen, Poaceae was generally high but decreased values in the most recent sample (range = 27–46%). Additionally, other herbaceous pollen taxa were present, including Asteraceae, which also increased in the most recent sample (range = 0–3%). Tree pollen taxa followed a similar pattern to AU7 with lower abundances characterized in the pre-modern samples by *Brachystegia* (mean = 6%) until the most recent sample, where *Podocarpus* and *Pinus* dominated (52%, 10%). Microcharcoal increased over an order of magnitude from the pre-modern (mean = 4,947 particles/cm<sup>3</sup>) to the modern samples (mean = 38,917 particles/cm<sup>3</sup>), with charcoal with high aspect ratios indicating a grassy source dominating.

The terrace samples presented in Figure 8D are a synthesis of pollen samples taken from profiles Kasitu 2, Kasitu 5, and Luwelezi terraces and range in age from 8ka to modern. The general patterns

TABLE 4 Quantities of stanols (ng/g<sub>g</sub>/g<sub>TOC</sub>) and the ratio (coprostanol + epi-coprostanol)/(5 $\beta$ -stigmastanol-3 $\beta$ -ol + 5 $\beta$ -stigmastanol-3 $\beta$ -ol) from AU7, Mzimba region, Malawi.

Sample number	Mean depths (cm)	Coprostanol (5 $\beta$ -cholestan-3 $\beta$ -ol) ( $\mu$ g/g <sub>TOC</sub> )	epi-Coprostanol (5 $\beta$ -cholestan-3 $\alpha$ -ol) ( $\mu$ g/g <sub>TOC</sub> )	5 $\beta$ -Stigmastanol (5 $\beta$ -stigmastanol-3 $\beta$ -ol) ( $\mu$ g/g <sub>TOC</sub> )	epi-5 $\beta$ -Stigmastanol (5 $\beta$ -stigmastanol-3 $\alpha$ -ol) ( $\mu$ g/g <sub>TOC</sub> )	Cholestanol (5 $\alpha$ -cholestan-3 $\beta$ -ol) ( $\mu$ g/g <sub>TOC</sub> )	Stigmastanol (5 $\alpha$ -stigmastanol-3 $\beta$ -ol) ( $\mu$ g/g <sub>TOC</sub> )	(Coprostanol+epi-coprostanol)/(5 $\beta$ -stigmastanol+epi-5 $\beta$ -stigmastanol)
ISO42	2.5	0.7	0.5	3.9	1.2	8.3	37	0.2
ISO43	15	0.1	0.1	1.6	0.7	6.2	17	0.1
ISO44	26.25	0.1	0.4	1.1	0.5	3.4	17	0.3
ISO45	33.75	0.2	0.2	1.4	0.7	4.5	13	0.2
ISO46	44	0.2	0.3	1.8	1.1	9.7	17	0.2
ISO47	53	1.4	1.3	3.7	1.9	8.0	19	0.5
ISO48	58	0.3	0.4	1.9	1.1	9.4	18	0.2
ISO48	58	0.3	0.4	1.9	1.1	9.5	18	0.2
ISO49	69.75	0.3	0.5	1.6	1.3	12.5	19	0.3
ISO50	80.5	0.5	0.6	1.5	1.7	9.4	18	0.3

in the pollen assemblages shows a dominance of trees, particularly Pinopsida undifferentiated (20–40%) until the last 2 kyr. Given that *Podocarpus* pollen is the only native genus in this class, it is likely this phase was dominated by *Podocarpus*. At 2 ka, there was a notable increase in herbaceous pollen taxa, especially Poaceae (60%). Finally, in the samples from the last 100 years, there is an increase in pollen of Pinosopida undifferentiated (55–60%) and other trees. As the *Pinus* was introduced within this window and auger samples observe an increase in this genus, it is likely that this last increase represents an increase in both gymnosperms in the last century.

## 5 Discussion

Our integrated archaeo-ecological investigation of the Mzimba region of northern Malawi indicates that there are critical ecological inflection points associated with different human settlement and subsistence regimes in the past. The stable isotopic composition of the sites demonstrates a clear inverse correlation between <sup>15</sup>N and <sup>13</sup>C values. From soils and sediments, more positive <sup>15</sup>N values and more negative <sup>13</sup>C values are indicative of higher concentrations of leaf litter and/or canopy, which biases the evapotranspiration of lighter isotopes (<sup>14</sup>N, <sup>12</sup>C) in the forms of NO<sub>2</sub> and CO<sub>2</sub> (Natelhoffer and Fry, 1988). Overall, the time-transgressive trend observed from the carbon isotopes studied ( $\delta^{13}\text{C}$ ) demonstrate a stronger tendency toward grassier landscape conditions from the start of the Holocene (Figure 6) with the caveat that the sample size is small before the Middle Holocene. However, these data are supported by the *n*-alkane data from AU7 (Figure 7) and pollen (Figure 8), which also show grass/herbaceous-dominant conditions, particularly within the last ~2 kyr.

Grass-dominant ecological niches that favour domesticated animals have been reconstructed across Africa correlating to the times when animal production is first documented in specific regions (Phelps et al., 2020). Farming and animal production are known to leave long legacies within soils on landscapes that can be measured from nutrient pools for millennia following site abandonment (Marshall, 2018; Cao et al., 2021; Storozum et al., 2021). The data from the Mzimba District have similarly left geochemical traces, supported by pollen data, indicating that human activities related to the introduction of agriculture also impacted land cover conditions, despite a lack of direct macro-archaeological evidence for the introduction of farming technologies at the sites we were testing. The oldest date for Iron Age agro-pastoralists in the Kasitu region is ca. 1.6 ka, which is taken from Munga Hill (Sinclair, 1991), ~1 km north of the Luwelezi profile (Robinson, 1982) and is similar to the oldest dates for food producers in Malawi from the southern part of the country (Juwayeyi, 2011).

Microarchaeological data indicates changing land cover conditions in relation to different land use strategies in the later Iron Age. Faecal biomarkers in the auger test adjacent to the HOR-1 site show increased input from omnivores during the period we interpret as representing initial food production at our test location, dating to around 1 ka. This was sustained until ca. 0.6 ka, when the *n*-alkane and pollen results show recovery of forest conditions and low presence of omnivores (in this case, humans). Omnivore

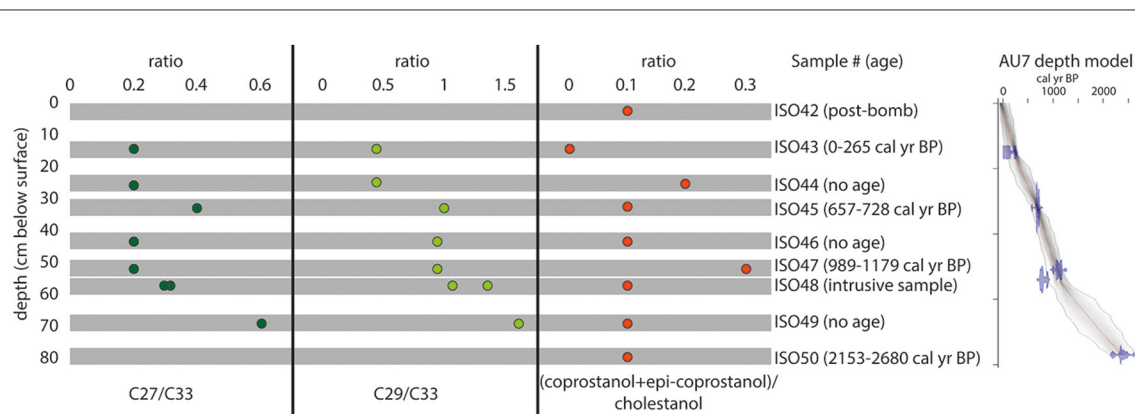


FIGURE 7

Ratios of the n-alkanes C27/C33 and C29/C33 on the left, with high values showing a higher input of biomass of broadleaf trees and low values a higher input of grasses and other herbaceous plants. Ratio of (coprostanol + epi-coprostanol)/cholestanol with high values characteristic for inputs of omnivorous faeces (likely from humans) from AU7, Mzimba region, Malawi.

populations then apparently rebounded and then increased further within the historical period. These patterns may indicate episodic settlement and land-use strategies in the second half of the Iron Age, or they may reflect a larger pattern of population decrease. Charcoal data from this sample in the core shows a slight increase in particle concentrations and some of the highest proportions of sedges, suggesting that waterlogged soils may have discouraged local cultivation and human occupation, while these activities continued outside the drainage catchment of the swale from which the core was collected.

The pollen and microcharcoal data are in general agreement with the other proxies studied, but they also indicate additional landscape formation processes that are important to the human ecology of the region. First, Cyperaceae pollen, reflecting wetland sedges, persisted throughout all periods of study and are evidence of continuation of seasonal wetland conditions in the studied locations from the Late Pleistocene to present (or nearly present) day. Second, increases in *Podocarpus* and *Pinus* (tree) taxa in the last 200 years occurred in the auger samples despite evidence for increased concentrations of microcharcoal, which is in general contrast to expected results based on simulated (Keane et al., 2004; D'Odorico et al., 2006; Phelps et al., 2020) and observed (Bakker et al., 2013; Marchant et al., 2018; Leunda et al., 2020) occurrences in ecological research. However, spatially and taxonomically complex ecological simulations challenge simplistic fire-driven forest-to-savannah formation models, demonstrating that fires consume saplings and seedlings that contribute negligibly to biomass (Hanan, 2008). Therefore, the presence of increased woody vegetation in combination with increased fire occurrence in the later phases of landscape formation in the Kasitu Valley are interpreted as reflecting spatially heterogeneous landscape management processes in which some patches of mature forest persisted at various points even as portions of the uplands adjacent to Luwelezi and Kasitu 5 rapidly eroded, presumably as an effect of forest cover loss. Of the 111 known species of *Pinus*, none are endemic to Africa south of the equator and only one species is recorded in tropical Asia (Price et al., 1998). Therefore, the presence of pines in Malawi, recorded in the pollen abundances from the

auger samples, is commonly understood to be an introduction associated with disturbance ecologies within the last 200–300 years (Richardson, 1998). It is also important to consider that pollen and microcharcoal are more often wind-borne than other proxies such as n-alkanes, faecal biomarkers and bulk stable isotopes, which likely reflect more localised vegetation conditions. Introduced *Pinus* stands are currently maintained on the Viphya Plateau immediately to the east of the Kasitu Valley.

Based on the total available evidence, the most significant ecological inflection point occurs in the Late Holocene at the time in which Iron Age agro-pastoralists are archaeologically identified in the region (Juwayeyi, 1981, 1991, 2008, 2011; Robinson, 1982; Davison, 1991). Although preservation of organic matter was variable and affects the robustness of the interpretations, the general indicators of plant and faunal ecologies corroborate sedimentation values, suggesting that after the introduction of farming techniques to this region of southern-central Africa, the landscape became generally more open and discharge from the uplands, where sediments are more prone to erosion, accelerated. More recent settlement (dating to within the last 75 years) shows accelerated modes of spatial heterogeneity with increasing abundances of *Podocarpus* pollen, while n-alkane and carbon isotope values show grassier ecological conditions predominate relative to samples analysed from the Middle Holocene and earlier.

Archaeological and ethnographic proxy data suggest that impacts in more recent times have influenced landscape formation in an accelerating manner. The presence of iron-working sites outside the rockshelters are not well dated and did not occur within the lifetimes of most residents of the Mzimba region, but residents over the age of 60 remember their elders talking about iron smelting. The bloomeries also appear to not have been abandoned for long periods of time, with some furnaces transitioning from nearly complete and standing in 2016 (at the onset of MALAPP) to a current state of collapse, corroborating ethnographic accounts. A radiocarbon age analysed from the inside of a tuyere at the HOR-1 site was determined to be  $40 \pm 25$  yr BP (cal AD 1816–1956; UGAMS-30619) indicating that smelting was ongoing into recent times. However, today the most

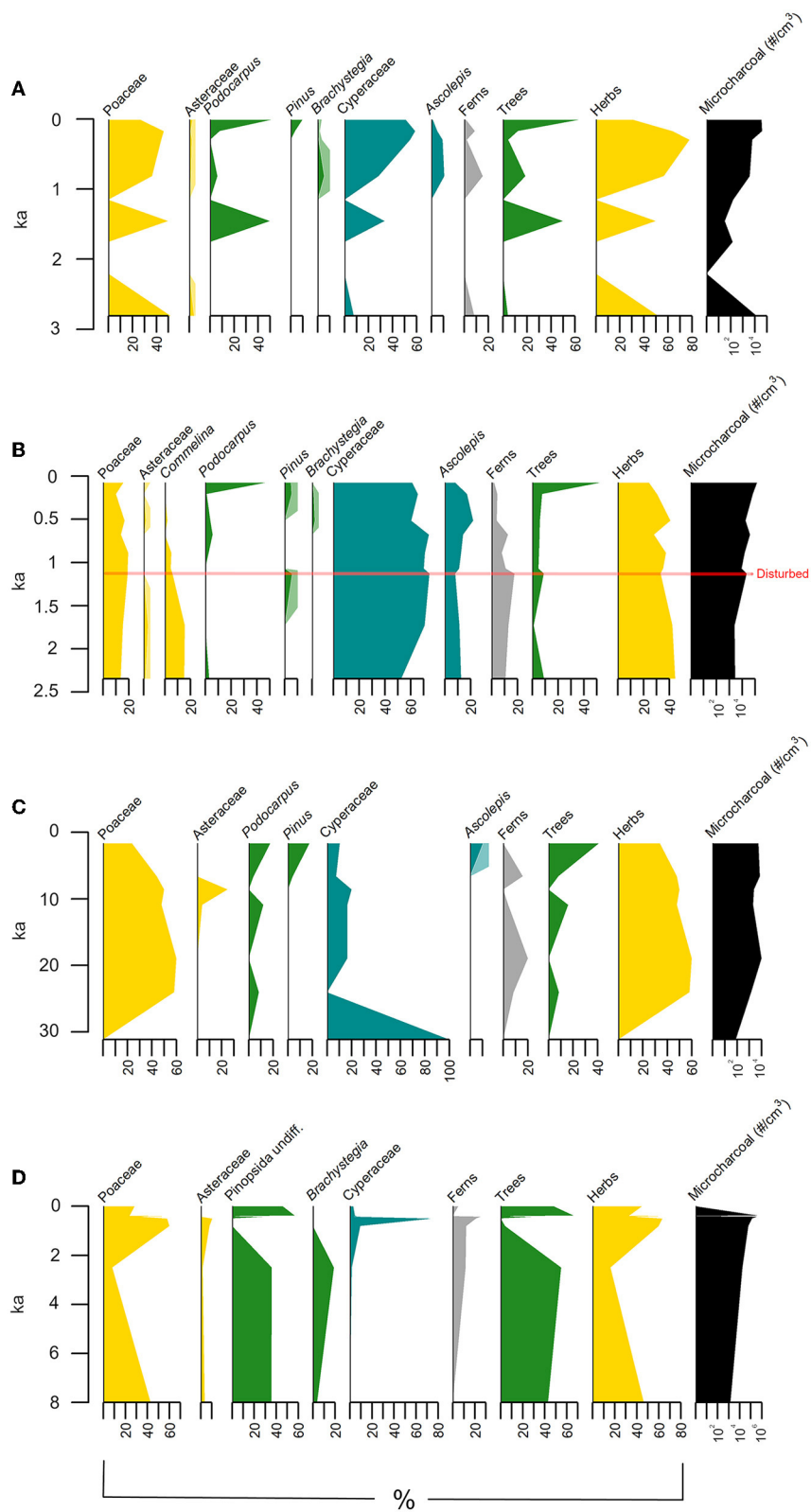


**FIGURE 8**  
 Fossil pollen from three sediment cores in the Mzimba region, Malawi. Darker shades inset within taxonomic categories indicate 5x percent value relative to the lighter shade. Sites included are (A) AU3, (B) AU7, (C) AU8 and (D) aggregated data from Kasitu 2, Kasitu 5, and Luwelezi terraces.



obvious local footprints of human environmental influence are firewood collecting and charcoal production which are supported by the  $^{13}\text{C}$  data, but the faecal biomarker data suggests that the number of people living (and/or defaecating) in the area is within or less than the general historical level. Thus, we interpret the current mosaic grassland/forest interspersed with seasonally flooded *dambos* in the Mt. Hora region to be a long-term legacy landscape with multiple stages of transition overprinted on prior anthropic states rather than an unprecedented historical ecological condition. Simultaneously, sedimentation rates even within the last ca. 0.4 kyr from the Kasitu terraces demonstrate that there has been another inflection point in erosion, sedimentation, and vegetation change over the historical period and accelerating into the present day.

## 6 Conclusion

Multiproxy biogenic data from the Mzimba region indicate that the region consisted of mixed woodland/grassland taxa during the terminal Pleistocene with an increase in woodland in the Early Holocene. Land cover transitioned to more open conditions by the Middle Holocene, which accords with increased evidence for fire, particularly after 3 ka, which is when the genetic replacement of hunter-gatherer-foragers with Bantu-speaking people ancestrally connected to modern populations occurs in the archaeological record (Skoglund et al., 2017; Lipson et al., 2022) and technologies associated with farming in this region are first documented (Robinson, 1982). Geomorphic and sedimentologic data from alluvial terraces support microarchaeological results indicating that fires and land clearance accelerated by ca. 1.2 ka and induced significant amounts of erosion of the uplands. Biomarkers prior to and during this period indicate an increase in human settlement next to the HOR-1 rockshelter and all proxies studied point to a transition to a more open, grassier landscape in the Late Holocene. Finally, afforestation associated with commercial timber farming of introduced pine species over the last several decades attest to ongoing anthropogenic impacts.

There is an apparent link between the novel introduction of farming and associated technologies and ecological changes exceeding the pace of natural climate variability alone. Our long human-ecological record supports the hypothesis that the formation of anthropogenic landscapes is temporally and conceptually divorced from the Industrial Revolution or other supposed stratigraphic markers of the Anthropocene, calling into question the epistemological value of this epoch outside the field of geochronology (Ruddiman et al., 2015; 2020; 2018). The data we present here demonstrate a notable processual connection between agro-pastoralism, erosion and vegetation change, which has left a clear footprint on the modern landscape. Although lacking in the global synchronicity of expression that comes from an extra-terrestrial meteor impact, the spread and intensification of farming technologies globally after 3 ka (Stephens, 2019; Morrison, 2021) is akin to other stratigraphic boundary events. For example, the Late Ordovician to Silurian transition or Early to Middle Pleistocene in the palaeontologic records are far more coarsely resolved, but also lack precise synchronicity and unfold correlatively and diachronically - just as global human impacts

on landscape formation due to intensive hunting and gathering, land domestication and globalisation processes can be ascertained today (Edgeworth et al., 2015; Williams et al., 2022). The results presented in this study underscore the complexity, heterogeneity, and overprinting of human impacts across landscapes with deep settlement histories.

## Data availability statement

The data and code presented in the article have been uploaded to the Figshare repository and can be accessed using the following doi: 10.6084/m9.figshare.23092127.

## Author contributions

DW, JT, SI, and JB contributed to conception and design of the study. JT, JD, DW, and PK conducted fieldwork and collected samples. Samples were analysed by DW, SI, JB, and J-HC. DW and BD organized the database and performed the statistical analyses. DW and JT wrote the first draft of the manuscript. DW, JT, SI, JB, and J-HC wrote sections of the manuscript. All authors contributed to manuscript revision, read, and approved the submitted version.

## Acknowledgments

The Malawi Department of Museums and Monuments provided permission for the research. Land access was facilitated by Paramount Chief Inkosi ya Makosi M'Mbelwa V, Inkosi Chindi, Inkosi Kampingo Sibande, Inkosana Thomas Nkosi, Mzimba Heritage Association, and the generosity of the Mzimba community. Sample recovery and preparation in the field was facilitated by participation from officials from the Malawi government, the Mzimba community, and students from Malawian and international universities. JT received funding for fieldwork and sample analysis from the Wenner-Gren Foundation (Grant no. 9437), the National Geographic Society, Yale University, and Hyde Family Foundations. DW received funding from a start-up grant from the University of Oslo for stable isotope and biomarker extractions and/or analytical costs. SI received funding from the National Science Foundation Division of Environmental Biology Grant #2049982. Stefanie Klassen provided technical assistance with the biomarker analyses at the University of Mainz. Vendela Bergin Hansen prepared the stable isotope samples for study and William Hagopian at the UiO CLIPT lab analysed the samples using EA-IRMS. The authors would like to thank editor Sjoerd Kluiwing and reviewers David Kaniewski and Harald Stollhofen for their comments and critiques, which improved the quality of the final manuscript.

## Conflict of interest

The authors declare that the research was conducted in the absence of any commercial or financial relationships that could be construed as a potential conflict of interest.

The author DW declared that they were an editorial board member of Frontiers, at the time of submission. This had no impact on the peer review process and the final decision.

## Publisher's note

All claims expressed in this article are solely those of the authors and do not necessarily represent those of their affiliated organizations, or those of the publisher, the editors and the

reviewers. Any product that may be evaluated in this article, or claim that may be made by its manufacturer, is not guaranteed or endorsed by the publisher.

## Supplementary material

The Supplementary Material for this article can be found online at: <https://www.frontiersin.org/articles/10.3389/fearc.2023.1250871/full#supplementary-material>

## References

- Ambrose, S. H. (1991). Effects of diet, climate and physiology on nitrogen isotope abundances in terrestrial foodwebs. *J. Archaeol. Sci.* 18, 293–317. doi: 10.1016/0305-4403(91)90067-Y
- Ausman, L. M. (1993). Fecal bile acids and neutral sterols in the cotton-top tamarin (*Saguinus oedipus*). *Comp. Biochem. Physiol.* 105, 655–663. doi: 10.1016/0305-0491(93)90102-B
- Bakker, J., Paulissen, E., Kaniewski, D., Poblome, J., De Laet, V., Verstraeten, G., et al. (2013). Climate, people, fire and vegetation: new insights into vegetation dynamics in the Eastern Mediterranean since the 1st century AD. *Climate Past* 9, 57–87. doi: 10.5194/cp-9-57-2013
- Beltrame, M. H., Rubel, M. A., and Tishkoff, S. A. (2016). Inferences of African evolutionary history from genomic data. *Curr. Opin. Genetic. Dev.* 41, 159–166. doi: 10.1016/j.gde.2016.10.002
- Bethell, P. H., Goad, L. J., Evershed, R. P., and Ottaway, J. (1994). The study of molecular markers of human activity: the use of coprostanol in the soil as an indicator of human faecal material. *J. Archaeol. Sci.* 21, 619–632. doi: 10.1006/jasc.1994.1061
- Bird, R. B., Bird, D. W., Coddling, B. F., Parker, C. H., Jones, J. H. (2008). The “fire stick farming” hypothesis: Australian Aboriginal foraging strategies, biodiversity, and anthropogenic fire mosaics. *Proc. Nat. Acad. Sci.* 105, 14796–14801. doi: 10.1073/pnas.0804757105
- Birk, J. J., Dippold, M., Wiesenberg, G. L. B., Glaser, B. (2012). Combined quantification of faecal sterols, stanols, stanones and bile acids in soils and terrestrial sediments by gas chromatography–mass spectrometry. *J. Chromatogr. A* 1242, 1–10. doi: 10.1016/j.chroma.2012.04.027
- Blaauw, M., and Christen, J. A. (2011). Flexible paleoclimate age-depth models using an autoregressive gamma process. *Bayesian Anal.* 6, 457–474. doi: 10.1214/ba/1339616472
- Boivin, N., and Crowther, A. (2021). Mobilizing the past to shape a better Anthropocene. *Nat. Ecol. Evol.* 5, 273–284. doi: 10.1038/s41559-020-01361-4
- Boivin, N. L., Zeder, M. A., Fuller, D. Q., Crowther, A., Larson, G., Erlandson, J. M., et al. (2016). Ecological consequences of human niche construction: examining long-term anthropogenic shaping of global species distributions. *Proc. Nat. Acad. Sci. U. S. A.* 113, 6388–6396. doi: 10.1073/pnas.1525200113
- Bonnefille, R., and Riollet, G. (1980). *Pollens des Savanes d'Afrique Orientale*. Paris: CNRS Editions.
- Bøtter-Jensen, L., Solongo, S., Murray, A. S., Banerjee, D., and Jungner, H. (2000). Using the OSL single-aliquot regenerative-dose protocol with quartz extracted from building materials in retrospective dosimetry. *Rad. Measur.* 32, 841–845. doi: 10.1016/S1350-4487(99)00278-4
- Bowling, D. R., Pataki, D. E., and Randerson, J. T. (2008). Carbon isotopes in terrestrial ecosystem pools and CO<sub>2</sub> fluxes. *New Phytol.* 178, 24–40. doi: 10.1111/j.1469-8137.2007.02342.x
- Braje, T. J., and Erlandson, J. M. (2013). Human acceleration of animal and plant extinctions: a late Pleistocene, Holocene, and Anthropocene continuum. *Anthropocene* 4, 14–23. doi: 10.1016/j.anucene.2013.08.003
- Breecker, D. O., Sharp, Z. D., and McFadden, L. D. (2010). Atmospheric CO<sub>2</sub> concentrations during ancient greenhouse climates were similar to those predicted for AD 2100. *Proc. Nat. Acad. Sci.* 107, 576–580. doi: 10.1073/pnas.0902323106
- Brovkin, V., Brook, E., Williams, J. W., Bathiany, S., Lenton, T. M., Barton, M., et al. (2021). Past abrupt changes, tipping points and cascading impacts in the Earth system. *Nat. Geosci.* 14, 550–558. doi: 10.1038/s41561-021-00790-5
- Buggle, B., Wiesenberg, G. L. B., and Glaser, B. (2010). Is there a possibility to correct fossil n-alkane data for postdepositional alteration effects? *Appl. Geochem.* 25, 947–957. doi: 10.1016/j.apgeochem.2010.04.003
- Bull, I. D., Evershed, R. P., and Betancourt, P. P. (2001). An organic geochemical investigation of the practice of manuring at a Minoan site on Psira Island, Crete. *Geoarchaeology* 16, 223–242. doi: 10.1002/1520-6548(200102)16:2andlt;223::AID-GEA1002andgt;3.0.CO;2-7
- Bull, I. D., Lockheart, M. J., Elhmmali, M. M., Roberts, D. J., and Evershed, R. P. (2002). The origin of faeces by means of biomarker detection. *Environ. Int.* 27, 647–654. doi: 10.1016/S0160-4120(01)00124-6
- Burrough, S. L., and Willis, K. J. (2015). Ecosystem resilience to late-Holocene climate change in the Upper Zambezi Valley. *The Holocene* 25, 1811–1828. doi: 10.1177/0959683615591355
- Bush, R. T., and McInerney, F. A. (2013). Leaf wax n-alkane distributions in and across modern plants: implications for paleoecology and chemotaxonomy. *Geochimica et Cosmochimica Acta* 117, 161–179. doi: 10.1016/j.gca.2013.04.016
- Campbell, B. M., Cunliffe, R. N., and Gambiza, J. (1995). Vegetation structure and small-scale pattern in Miombo Woodland, Marondera, Zimbabwe. *Bothalia* 25, 121–126. doi: 10.4102/abc.v25i1.721
- Cao, B., Yu, L., Li, X., Chen, M., Li, X., Hao, P., et al. (2021). A 1 km global cropland dataset from 10 000 BCE to 2100 CE. *Earth Syst. Sci. Data* 13, 5403–5421. doi: 10.5194/essd-13-5403-2021
- Castañeda, I. S., Werne, J. P., Johnson, T. C., and Filley, T. R. (2009). Late Quaternary vegetation history of southeast Africa: the molecular isotopic record from Lake Malawi. *Palaeogeogr. Palaeoclimatol. Palaeoecol.* 275, 100–112. doi: 10.1016/j.palaeo.2009.02.008
- Castañeda, I. S., Werne, J. P., Johnson, T. C., and Powers, L. A. (2011). Organic geochemical records from Lake Malawi (East Africa) of the last 700 years, part II: biomarker evidence for recent changes in primary productivity. *Palaeogeogr. Palaeoclimatol. Palaeoecol.* 303, 140–154. doi: 10.1016/j.palaeo.2010.01.006
- Cerling, T. E., Quade, J., Wang, Y., and Bowman, J. R. (1989). Carbon isotopes in soils and palaeosols as ecology and palaeoecology indicators. *Nature* 341, 138–139. doi: 10.1038/341138a0
- Chesworth, W., Camps Arbustain, M., Macías, F., and Spaargaren, O. (2008). “Cambisols,” in *Encyclopedia of Soil Science*, ed W. Chesworth (Dordrecht: Springer Netherlands), 80–81.
- Chevalier, M., and Chase, B. M. (2015). Southeast African records reveal a coherent shift from high- to low-latitude forcing mechanisms along the east African margin across last glacial–interglacial transition. *Quarter. Sci. Rev.* 125, 117–130. doi: 10.1016/j.quascirev.2015.07.009
- Clark, J. D. (1956). Prehistory in Nyasaland. *Nyasaland J.* 9, 92–119.
- Commisso, R. G., and Nelson, D. E. (2006). Modern plant  $\delta^{15}N$  values reflect ancient human activity. *J. Archaeol. Sci.* 33, 1167–1176. doi: 10.1016/j.jas.2005.12.005
- Davison, S. (1991). Namaso: a newly-defined cultural entity of the late first millennium AD, and its place in the iron age sequence of southern Malawi. *Azania Archaeol. Res. Africa* 26, 13–62. doi: 10.1080/00672709109511424
- DeBusk, J., and George, H. (1998). A 37,500-year pollen record from lake malawi and implications for the biogeography of afro-montane forests. *J. Biogeogr.* 25, 479–500. doi: 10.1046/j.1365-2699.1998.2530479.x
- D'Odorico, P., Laio, F., and Ridolfi, L. (2006). A probabilistic analysis of fire-induced tree-grass coexistence in savannas. *The Am. Natur.* 167, E79–E87. doi: 10.1086/500617
- Dussubieux, L., Welling, M., and Kaliba, P. (2023). European trade in Malawi: the glass bead evidence. *Afr. Archaeol. Rev.* 40, 377–396. doi: 10.1007/s10437-022-09486-6
- Ebelhar, S. A., Chesworth, W., Paris, Q., et al. (2008). “Lixisols,” *Encyclopedia of Soil Science*, ed W. Chesworth (Dordrecht: Springer Netherlands), 439–440.
- Edgeworth, M., deB Richter, D., Waters, C., Haff, P., Neal, C., and Price, S. J. (2015). Diachronous beginnings of the anthropocene: the lower bounding surface of anthropogenic deposits. *The Anthr. Rev.* 2, 33–58. doi: 10.1177/2053019614565394

- Eglinton, G., and Hamilton, R. J. (1967). Leaf epicuticular waxes. *Science* 156, 1322–1335. doi: 10.1126/science.156.3780.1322
- Ellis, E. C., Gauthier, N., Goldewijk, K. K., Bird, R. B., Boivin, N., Diaz, S., et al. (2021). People have shaped most of terrestrial nature for at least 12,000 years. *Proc. Nat. Acad. Sci.* 118, e2023483118. doi: 10.1073/pnas.2023483118
- Ellis, E. C. (2011). Anthropogenic transformation of the terrestrial biosphere. *Philos. Trans. Royal Soc. Mathematic. Phys. Eng. Sci.* 369, 1010–1035. doi: 10.1098/rsta.2010.0331
- Evershed, R. P. (2008). Organic residue analysis in archaeology: the archaeological biomarker revolution. *Archaeometry* 50, 895–924. doi: 10.1111/j.1475-4754.2008.00446.x
- Evershed, R. P., Bethell, P. H., Reynolds, P. J., and Walsh, N. J. (1997). 5 $\beta$ -stigmastanol and related 5 $\beta$ -stanols as biomarkers of manuring: analysis of modern experimental material and assessment of the archaeological potential. *J. Archaeol. Sci.* 24, 485–495. doi: 10.1006/jasc.1996.0132
- Fægri, K., Kaland, P. E., and Krzywinski, K. (1989). *Textbook of Pollen Analysis*. Chichester: John Wiley and Sons Ltd.
- Fan, S., Spence, J. P., Feng, Y., Hansen, M. E. B., Terhorst, J., Beltrame, M. H., et al. (2023). Whole-genome sequencing reveals a complex African population demographic history and signatures of local adaptation. *Cell* 186, 923–939.e914. doi: 10.1016/j.cell.2023.01.042
- Feakins, S. J., Liddy, H. M., Tauxe, L., Galy, V., Feng, X., Tierney, J. E., et al. (2020). Miocene C4 grassland expansion as recorded by the Indus Fan. *Paleoceanogr. Paleoclimatol.* 35, e2020PA003856. doi: 10.1029/2020PA003856
- Frost, P. (1996). “The ecology of miombo woodlands,” in *The Miombo in Transition: Woodlands and Welfare in Africa*, ed B. Campbell (Bogor: Centre for International Forestry Research), 11–57.
- Garcin, Y., Vincens, A., Williamson, D., Buchet, G., and Guiot, J. (2007). Abrupt resumption of the African Monsoon at the Younger Dryas—Holocene climatic transition. *Q. Sci. Rev.* 26, 690–704. doi: 10.1016/j.quascirev.2006.10.014
- Garrity, D., Dixon, J., and Boffa, J. M. (2012). *Understanding African Farming Systems: Science and Policy Implications*. Sydney: Australian International Food Security Centre.
- Gill, F. L., Dewhurst, R. J., Dungait, J. A., Evershed, R. P., Ives, L., Li, C. S., et al. (2010). Archaeol – a biomarker for foregut fermentation in modern and ancient herbivorous mammals? *Organic Geochem.* 41, 467–472. doi: 10.1016/j.orggeochem.2010.02.001
- Hanan, N. P., Sea, W. B., Dangelmayr, G., Govender, N. (2008). Do fires in savannas consume woody biomass? A comment on approaches to modeling savanna dynamics. *The Am. Nat.* 171, 851–856. doi: 10.1086/587527
- Hoefs, M. J. L., Rijpstra, W. I. C., and Sinnighe Damsté, J. S. (2002). The influence of oxic degradation on the sedimentary biomarker record I: evidence from Madeira Abyssal Plain turbidites. *Geochimica et Cosmochimica Acta* 66, 2719–2735. doi: 10.1016/S0016-7037(02)00864-5
- Högberg, P. (1997). Tansley review No. 95 - <sup>15</sup>N natural abundance in soil-plant systems. *New Phytol.* 137, 179–203. doi: 10.1046/j.1469-8137.1997.00808.x
- Hogg, A. G., Heaton, T. J., Hua, Q., Palmer, J. G., Turney, C. S., Southon, J., et al. (2020). SHCal20 southern hemisphere calibration, 0–55,000 years cal BP. *Radiocarbon* 62, 759–778. doi: 10.1017/RDC.2020.59
- Hopkins, D. A. S. (1973). *The Geology of the Rumph–Nkhata Bay Area. Bulletin 38/39*. Zomba: Ministry of Agriculture and Natural Resources, Geological Survey Department.
- IUSS Working Group WRB (2015) *World Reference Base for Soil Resources 2014, Update 2015. International soil Classification System for Naming Soils and Creating Legends for Soil Maps*. Rome: World Soil Resources Reports No. 106. Food and Agriculture Organization of the United Nations.
- Ivory, S. J., Lézine, A.-M., Vincens, A., Cohen, A. S. (2018). Waxing and waning of forests: late quaternary biogeography of the Lake Malawi region, southeast Africa. *Global Change Biol.* 24, 2939–2951. doi: 10.1111/gcb.14150
- Ivory, S. J., Lézine, A. M., Vincens, A., and Cohen, A. S. (2012). Effect of aridity and rainfall seasonality on vegetation in the southern tropics of East Africa during the Pleistocene/Holocene transition. *Q. Res.* 77, 77–86. doi: 10.1016/j.yqres.2011.11.005
- Jackson, G. (1968). The vegetation of Malawi. II. The *Brachystegia* woodlands X. *Brachystegia* with evergreen understorey. *The Soc. Malawi J.* 21, 11–19.
- Jackson, G. (1974). Cryptogean germination and other seedling adaptations to the burning of vegetation in savanna regions: the origin of the pyrophytic habit. *New Phytol.* 73, 771–780. doi: 10.1111/j.1469-8137.1974.tb01305.x
- Juggins, S. (2022). *Rioja: Analysis of Quaternary Science Data*. Available online at: <https://cran.r-project.org/package=rioja> (accessed June 29, 2023).
- Juwayeyi, Y. M. (1981). *The Later Prehistory of Southern Malawi: A Contribution to the Study of Technology and Economy During the Later Stone Age and Iron Age Periods*. Berkeley, CA: University of California, Berkeley.
- Juwayeyi, Y. M. (1991). Late iron age burial practices in the southern Lake Malawi area. *The South Afr. Archaeol. Bull.* 46, 25–33. doi: 10.2307/3889010
- Juwayeyi, Y. M. (2008). “Human and animal interaction on the shire highlands, Malawi: the evidence from malowa rockshelter,” in *Animals and People: Archaeozoological Papers in Honour of Ina Plug*, eds S. Badenhorst, P. Mitchell, and J. C. Driver (Oxford: Archaeopress).
- Juwayeyi, Y. M. (2011). Ecological pressure and the transition from foraging to agricultural lifestyle on the Shire Highlands, Malawi. *Hum. Ecol.* 39, 361–371. doi: 10.1007/s10745-011-9391-1
- Juwayeyi, Y. M. (2020). *Archaeology and Oral Tradition in Malawi: Origins and Early History of the Chewa*. Suffolk: Boydell and Brewer.
- Keane, R. E., Cary, G. J., Davies, I. D., Flannigan, M. D., Gardner, R. H., Lavorel, S., et al. (2004). A classification of landscape fire succession models: spatial simulations of fire and vegetation dynamics. *Ecol. Modell.* 179, 3–27. doi: 10.1016/j.ecolmodel.2004.03.015
- Kindt, R., Lillesø, J. P. B., van Breugel, P., et al. (2014). *Potential Natural Vegetation of Eastern Africa (Ethiopia, Kenya, Malawi, Rwanda, Tanzania, Uganda and Zambia)*. Copenhagen: Department of Geoscience and Natural Resource Management, University of Copenhagen.
- Konecky, B. L., Russell, J. M., Johnson, T. C., Brown, E. T., Berke, M. A., Werne, J. P., et al. (2011). Atmospheric circulation patterns during late Pleistocene climate changes at Lake Malawi, Africa. *Earth Planetar. Sci. Lett.* 312, 318–326. doi: 10.1016/j.epsl.2011.10.020
- Kottek, M., Grieser, J., Beck, C., Rudolf, B., and Rubel, F. (2006). World map of the Köppen-Geiger climate classification updated. *Meteorol. Zeitschrift* 15, 259–263. doi: 10.1127/0941-2948/2006/0130
- Leeming, R., Ball, A., Ashbolt, N., and Nichols, P. (1996). Using faecal sterols from humans and animals to distinguish faecal pollution in receiving waters. *Water Res.* 30, 2893–2900. doi: 10.1016/S0043-1354(96)00011-5
- Lenton, T. M. (2013). Environmental tipping points. *Ann. Rev. Environ. Resour.* 38, 1–29. doi: 10.1146/annurev-environ-102511-084654
- Leunda, M., Gil-Romera, G., Daniau, A. L., Benito, B. M., and González-Sampériz, P. (2020). Holocene fire and vegetation dynamics in the Central Pyrenees (Spain). *CATENA* 188, 104411. doi: 10.1016/j.catena.2019.104411
- Li, G., Messina, J. P., Peter, B. G., and Snapp, S. S. (2017). Mapping land suitability for agriculture in Malawi. *Land Degr. Dev.* 28, 2001–2016. doi: 10.1002/ldr.2723
- Lipson, M., Sawchuk, E. A., Thompson, J. C., Oppenheimer, J., Tryon, C. A., and Ranhorn, K. L. (2022). Ancient DNA and deep population structure in sub-Saharan African foragers. *Nature* 603, 290–296. doi: 10.1038/s41586-022-04430-9
- Liritzis, I., Stamoulis, K., Papachristodoulou, C., and Ioannides, K. (2013). A re-evaluation of radiation dose-rate conversion factors. *Mediterranean Archaeol. Archaeometr.* 13, 1–15. Available online at: <https://www.maajournal.com/index.php/maa/article/view/1012>
- Maley, J. (1970). Contributions à l'étude du Bassin tchadien Atlas de pollens du Tchad. *Bullet. Nat. Plant. België* 40, 29–48. doi: 10.2307/3667543
- Marchant, R., Richer, S., Boles, O., Capitani, C., Courtney-Mustaphi, C. J., and Lane, P. (2018). Drivers and trajectories of land cover change in East Africa: human and environmental interactions from 6000 years ago to present. *Earth-Sci. Rev.* 12, 10. doi: 10.1016/j.earscirev.2017.12.010
- Marshall, F., Reid, R. E. B., Goldstein, S., Storozum, M., Wreschnig, A., Hu, L., et al. (2018). Ancient herders enriched and restructured African grasslands. *Nature* 561, 387–390. doi: 10.1038/s41586-018-0456-9
- Meadows, M. E. (1984a). Late quaternary vegetation history of the Nyika Plateau, Malawi. *J. Biogeogr. phy* 11, 209–222. doi: 10.2307/2844640
- Meadows, M. E. (1984b). Contemporary pollen spectra and vegetation of the Nyika Plateau, Malawi. *J. Biogeogr.* 11, 223–233. doi: 10.2307/2844641
- Miao, Y., Wu, F., Warny, S., Fang, X., Lu, H., and Fu, B. (2019). Miocene fire intensification linked to continuous aridification on the Tibetan Plateau. *Geology* 47, 303–307. doi: 10.1130/G45720.1
- Miller, J. M., Keller, H. M., Heckel, C., Kaliba, P. M., and Thompson, J. C. (2021). Approaches to land snail shell bead manufacture in the Early Holocene of Malawi. *Archaeol. Anthropol. Sci.* 13, 37. doi: 10.1007/s12520-021-01274-8
- Morris, B. (2006). The ivory trade and chiefdoms in pre-colonial Malawi. *The Soc. Malawi J.* 59, 6–23. Available online at: <https://www.jstor.org/stable/29797210>
- Morrison, K. D., Hammer, E., Boles, O., Madella, M., Whitehouse, N., Gaillard, M.-J., et al. (2021). Mapping past human land use using archaeological data: a new classification for global land use synthesis and data harmonization. *PLoS ONE* 16, e0246662. doi: 10.1371/journal.pone.0246662
- Murray, A. S., and Wintle, A. G. (2003). The single aliquot regenerative dose protocol: Potential for improvements in reliability. *Rad. Measur.* 37, 377–381. doi: 10.1016/S1350-4487(03)00053-2
- Natelhofer, K. J., and Fry, B. (1988). Controls on natural nitrogen-15 and carbon-13 abundances in forest soil organic matter. *Soil Sci. Soc. Am. J.* 52, 1633–1640. doi: 10.2136/sssaj1988.03615995005200060024x
- NOAA (2022). *Global Climate Normals, Mzimba Station Record 67485*. Asheville, North Carolina, USA.

- Paz, C. G., Rodríguez, T. T., Behan-Pelletier, V. M., et al. (2008). "Ferralsols," in *Encyclopedia of Soil Science*, ed W. Chesworth (Dordrecht: Springer Netherlands), 237–240.
- Phelps, L. N., Broennimann, O., Manning, K., Timpson, A., Jousse, H., Mariethoz, G., et al. (2020). Reconstructing the climatic niche breadth of land use for animal production during the African Holocene. *Glob. Ecol. Biogeogr.* 29, 127–147. doi: 10.1111/geb.13015
- Pinter, N., Fiedel, S., and Keeley, J. E. (2011). Fire and vegetation shifts in the Americas at the vanguard of Paleoindian migration. *Q. Sci. Rev.* 30, 269–272. doi: 10.1016/j.quascirev.2010.12.010
- Potts, R. (1998). Environmental hypotheses of hominin evolution. *Yearbook Phys. Anthropol.* 41, 93–136. doi: 10.1002/(SICI)1096-8644(1998)107:27+andlt;93::AID-AJPA5andgt;3.0.CO;2-X
- Prescott, J. R., and Hutton, J. T. (1994). Cosmic ray contributions to dose rates for luminescence and ESR dating: large depths and long-term time variations. *Rad. Measur.* 23, 497–500. doi: 10.1016/1350-4487(94)90086-8
- Price, R. A., Liston, A., and Strauss, S. H. (1998). "Phylogeny and systematics of Pinus," in *Ecology and Biogeography of Pinus*, eds D. M. Richardson (Cambridge: Cambridge University Press), 49–68.
- Prost, K., Birk, J. J., Lehndorff, E., Gerlach, R., Amelung, W. (2017). Steroid biomarkers revisited – Improved source identification of faecal remains in archaeological soil material. *PLoS ONE* 12, e0164882. doi: 10.1371/journal.pone.0164882
- R Core Team (2023). *R: A Language and Environment for Statistical Computing*. Vienna: R Foundation for Statistical Computing.
- Richardson, D. M. (1998). Forestry trees as invasive aliens. *Conserv. Biol.* 12, 18–26. doi: 10.1111/j.1523-1739.1998.96392.x
- Roberts, P., Hunt, C., Arroyo-Kalin, M., Evans, D., and Boivin, N. (2017). The deep human prehistory of global tropical forests and its relevance for modern conservation. *Nat. Plants* 3, 17093. doi: 10.1038/nplants.2017.93
- Robinson, J. R., and Rowan, J. (2017). Holocene paleoenvironmental change in southeastern Africa (Makwe Rockshelter, Zambia): implications for the spread of pastoralism. *Q. Sci. Rev.* 156, 57–68. doi: 10.1016/j.quascirev.2016.11.030
- Robinson, K. S. R. (1982). *Iron Age of Northern Malawi: An Archaeological Reconnaissance*. Lilongwe: Malawi Govt. Ministry of Education and Culture.
- Ruddiman, W. F. (2013). The Anthropocene. *Ann. Rev. Earth Planetar. Sci.* 41, 45–68. doi: 10.1146/annurev-earth-050212-123944
- Ruddiman, W. F. (2018). Three flaws in defining a formal 'Anthropocene'. *Progr. Phys. Geogr. Earth Environ.* 42, 451–461. doi: 10.1177/0309133318783142
- Ruddiman, W. F., Ellis, E. C., Kaplan, J. O., and Fuller, D. Q. (2015). Defining the epoch we live in. *Science* 348, 38–39. doi: 10.1126/science.aaa7297
- Ruddiman, W. F., He, F., Vavrus, S. J., and Kutzbach, J. E. (2020). The early anthropogenic hypothesis: a review. *Q. Sci. Rev.* 240, 106386. doi: 10.1016/j.quascirev.2020.106386
- Ruiz Pessenda, L. C. R., De Oliveira, P. E., Mofatto, M., de Medeiros, V. B., Garcia, R. J. F., Aravena, R., et al. (2009). The evolution of a tropical rainforest/grassland mosaic in southeastern Brazil since 28,000 14C yr BP based on carbon isotopes and pollen records. *Q. Res.* 71, 437–452. doi: 10.1016/j.yqres.2009.01.008
- Schefeuf, E., Kuhlmann, H., Mollenhauer, G., Prange, M., Pätzold, J. (2011). Forcing of wet phases in southeast Africa over the past 17,000 years. *Nature* 480, 509–512. doi: 10.1038/nature10685
- Schoenberger, P. J., Wysocki, D. A., Benham, E. C., et al. (2012). *Field Book for Describing and Sampling Soils, Version 3, 0*. Lincoln: Natural Resources Conservation Service, National Soil Survey Center.
- Shah, V. G., Dunstan, R. H., Geary, P. M., Coombes, P., Roberts, T. K., Von Nagy-Felsobuki, E. (2007). Evaluating potential applications of faecal sterols in distinguishing sources of faecal contamination from mixed faecal samples. *Water Res.* 41, 3691–3700. doi: 10.1016/j.watres.2007.04.006
- Sinclair, P. J. J. (1991). Archaeology in eastern Africa: an overview of current chronological issues. *J. Afr. History* 32, 179–219. doi: 10.1017/S0021853700025706
- Sistiaga, A., Wrangham, R., Rothman, J. M., Summons, R. E. (2015). New insights into the evolution of the human diet from faecal biomarker analysis in wild chimpanzee and gorilla faeces. *PLoS ONE* 10, e0128931. doi: 10.1371/journal.pone.0128931
- Skoglund, P., Thompson, J. C., Prendergast, M. E., Mittnik, A., Sirak, K., Hajdinjak, M., et al. (2017). Reconstructing prehistoric African population structure. *Cell* 171, 59–71.e21. doi: 10.1016/j.cell.2017.08.049
- Snitker, G., Roos, C. I., 3rd, A. P. S., Maezumi, S. Y., Bird, D. W., Coughlan, M. R., et al. (2022). A collaborative agenda for archaeology and fire science. *Nat. Ecol. Evol.* 6, 835–839. doi: 10.1038/s41559-022-01759-2
- Soil Survey Staff. (1999) *Soil Taxonomy: A Basic System of Soil Classification for Making and Interpreting Soil Surveys*. Washington, DC: United States Department of Agriculture, Natural Resources Conservation Service.
- Srivastava, P. (2001). Paleoclimatic implications of pedogenic carbonates in Holocene soils of the Gangetic Plains, India. *Palaeogeogr. Palaeoclimatol. Palaeoecol.* 172, 207–222. doi: 10.1016/S0031-0182(01)00276-0
- Stephens, L., Fuller, D., Boivin, N., Rick, T., Gauthier, N., Kay, A., et al. (2019). Archaeological assessment reveals Earth's early transformation through land use. *Science* 365, 897. doi: 10.1126/science.aax1192
- Storozum, M. J., Goldstein, S. T., Contreras, D. A., Gidna, A. O., Mabulla, A. Z., Grillo, K. M., et al. (2021). The influence of ancient herders on soil development at Luxmanda, Mbulu Plateau, Tanzania. *CATENA* 204, 105376. doi: 10.1016/j.catena.2021.105376
- Subbiah, M. T. R., Kottke, B. A., and Jones, C. M. (1972). Nature of sterols excreted by non-human primates: Faecal sterols of baboon and rhesus monkey. *Int. J. Biochem.* 3, 430–436. doi: 10.1016/0020-711X(72)90094-8
- Thevenon, F., Williamson, D., Vincens, A., Taieb, M., Merdaci, O., Decobert, M., et al. (2003). A late-Holocene charcoal record from Lake Masoko, SW Tanzania: climatic and anthropologic implications. *The Holocene* 13, 785–792. doi: 10.1191/0959683603hl665rr
- Thompson, J. C., Wright, D. K., Ivory, S. J., Choi, J. H., Nightingale, S., Mackay, A., et al. (2021). Early human impacts and ecosystem reorganization in southern-central Africa. *Sci. Adv.* 7, eabf9776. doi: 10.1126/sciadv.abf9776
- Thompson, T. J. (1981). The origins, migration, and settlement of the northern Ngoni. *The Soc. Malawi J.* 34, 6–35.
- Tyagi, P., Edwards, D. R., and Coyne, M. S. (2008). Use of sterol and bile acid biomarkers to identify domesticated animal sources of fecal pollution. *Water Air Soil Pollut.* 187, 263–274. doi: 10.1007/s11270-007-9514-x
- Tylianakis, J. M., and Coux, C. (2014). Tipping points in ecological networks. *Trends Plant Sci.* 19, 281–283. doi: 10.1016/j.tplants.2014.03.006
- USGS (2018a) *USGS EROS Archive - Land Cover Products - Global Land Cover Characterization (GLCC) Version 1*. Sioux Falls, SD: United States Geological Survey Earth Resources Observation and Science Center.
- USGS (2018b) *USGS EROS Archive - Digital Elevation - Global 30 Arc-Second Elevation (GTOPO30)*. Sioux Falls, SD: United States Geological Survey Earth Resources Observation and Science Center.
- van Der Kaars, S., Miller, G. H., Turney, C. S., Cook, E. J., Nürnberg, D., Schönfeld, J., et al. (2017). Humans rather than climate the primary cause of Pleistocene megafaunal extinction in Australia. *Nat. Commun.* 8, 14142. doi: 10.1038/ncomms14142
- van der Lubbe, H. J. L., Frank, M., Tjallingii, R., and Schneider, R. R. (2016). Neodymium isotope constraints on provenance, dispersal, and climate-driven supply of Zambesi sediments along the Mozambique Margin during the past ~45,000 years. *Geochem. Geophys. Geosyst.* 17, 181–198. doi: 10.1002/2015GC006080
- Vicente, M., and Schlebusch, C. M. (2020). African population history: an ancient DNA perspective. *Curr. Opin. Genet. Dev.* 62, 8–15. doi: 10.1016/j.gde.2020.05.008
- Vincens, A., Williamson, D., Thevenon, F., Taieb, M., Buchet, G., Decobert, M., et al. (2003). Pollen-based vegetation changes in southern Tanzania during the last 4200 years: climate change and/or human impact. *Palaeogeogr. Palaeoclimatol. Palaeoecol.* 198, 321–334. doi: 10.1016/S0031-0182(03)00473-5
- Werger, M. J. A., and Coetzee, B. J. (1978). "The Sudano-Zambezian Region," in *Biogeography and Ecology of Southern Africa*, ed M. J. A. Werger (*The Hague: Dr W Junk bv Publishers*), 301–462.
- West, J. B., Bowen, G. J., Cerling, T. E., and Ehleringer, J. R. (2006). Stable isotopes as one of nature's ecological recorders. *Trends Ecol. Evol.* 21, 408–414. doi: 10.1016/j.tree.2006.04.002
- Williams, M., Leinfelder, R., Barnosky, A. D., Head, M. J., McCarthy, F. M., Cearreta, A., et al. (2022). Planetary-scale change to the biosphere signalled by global species translocations can be used to identify the Anthropocene. *Palaeontology* 65, e12618. doi: 10.1111/pala.12618
- Wright, D. K. (2022). Impact of farming on African landscapes. *The Anthr. Rev.* 10, 636–663. doi: 10.1177/20530196221140145
- Wright, D. K., MacEachern, S., Ambrose, S. H., Choi, J., Choi, J. H., Lang, C., et al. (2019). Iron Age landscape changes in the Benoué River Valley, Cameroon. *Q. Res.* 92, 323–339. doi: 10.1017/qua.2019.25
- Zech, M., Bugge, B., Leiber, K., Marković, S., Glaser, B., Hambach, U., et al. (2010). Reconstructing Quaternary vegetation history in the Carpathian Basin, SE-Europe, using n-alkane biomarkers as molecular fossils: problems and possible solutions, potential and limitations. *E. G. Q. Sci. J.* 58, 148–155. doi: 10.3285/eg.58.2.03
- Zech, M., and Glaser, B. (2008). Improved compound-specific  $\delta^{13}C$  analysis of n-alkanes for application in palaeoenvironmental studies. *Rapid Commun. Mass Spectr.* 22, 135–142. doi: 10.1002/rcm.3342
- Zocatelli, R., Lavrieux, M., Guillemot, T., Chassiot, L., Le Milbeau, C., and Jacob, J. (2017). Faecal biomarker imprints as indicators of past human land uses: source distinction and preservation potential in archaeological and natural archives. *J. Archaeol. Sci.* 81, 79–89. doi: 10.1016/j.jas.2017.03.010